

Bulk viscosity in 2SC quark matter

Mark G. Alford^{1,*} and Andreas Schmitt^{1,†}

¹*Department of Physics, Washington University St Louis, MO, 63130, USA*

(Dated: November 2, 2006)

The bulk viscosity of three-flavor color-superconducting quark matter originating from the non-leptonic process $u + s \leftrightarrow u + d$ is computed. It is assumed that up and down quarks form Cooper pairs while the strange quark remains unpaired (2SC phase). A general derivation of the rate of strangeness production is presented, involving contributions from a multitude of different subprocesses, including subprocesses that involve different numbers of gapped quarks as well as creation and annihilation of particles in the condensate. The rate is then used to compute the bulk viscosity as a function of the temperature, for an external oscillation frequency typical of a compact star r -mode. We find that, for temperatures far below the critical temperature T_c for 2SC pairing, the bulk viscosity of color-superconducting quark matter is suppressed relative to that of unpaired quark matter, but for $T \gtrsim T_c/30$ the color-superconducting quark matter has a higher bulk viscosity. This is potentially relevant for the suppression of r -mode instabilities early in the life of a compact star.

PACS numbers: 12.38.Mh,24.85.+p,26.60.+c

I. INTRODUCTION

Compact stars consist of extremely dense matter, part or all of which may be deconfined quark matter [1]. Quark matter that is sufficiently dense and cold is expected to be in a color-superconducting state [2], characterized by Cooper pairing between the quarks, mediated by their attractive strong interaction. This is analogous to the formation of electron Cooper pairs in a superconducting metal [3]. However, unlike electrons, quarks occur in many varieties: there are three colors and in a compact star core we expect to find three flavors, so a multitude of pairing (and thus symmetry breaking) patterns and hence different phases is theoretically possible [4]. It is an open problem of current research to determine the ground state out of these many possibilities for quark matter inside a compact star.

One approach to this problem is purely theoretical, using perturbative QCD as well as more phenomenological models in order to compare different possibilities and find the one with the lowest free energy. This approach yields a definite answer for very large densities (more precisely for quark chemical potentials μ much larger than the masses of the up, down, and strange quarks). In this situation, quark matter is in the color-flavor locked (CFL) state [5]. However, in nature, i.e., in the interior of a compact star, the quark chemical potential is expected to be of the order of 500 MeV or less, which requires the mass of the strange quark m_s to be taken into account. Moreover, further constraints on the matter are imposed by electric and color charge neutrality as well as by equilibrium with respect to the weak interaction. All these conditions impose a stress on the pairing, no matter which pairing pattern is chosen [6]. Therefore, besides the CFL phase, many unconventional color-superconducting phases have been proposed, e.g., phases that break rotational [7] or translational [8] symmetries.

The second approach to determining the ground state of dense quark matter in a compact star is the study of possible astrophysical effects of color superconductors. In particular, the ultimate goal is to compare observational data with theoretical predictions for color superconductors in order to exclude or confirm proposed phases. Moreover, one would like to use observations to distinguish between quark matter and more conventional matter inside the star, such as nuclear or hyperonic matter. Promising physical properties that are distinct for different color-superconducting phases are related to transport properties such as thermal conductivity [11], neutrino emissivity [12–15], magnetic fields [9, 10], and viscosity.

In this paper, we calculate the bulk viscosity of color-superconducting quark matter in the 2SC phase. (For a recent study of the bulk viscosity in spin-one color superconductors, see Ref. [16]; for hybrid/CFL matter see Ref. [17].). In 2SC quark matter, up and down quarks form Cooper pairs with each other while the strange quarks remain unpaired. Although constraints of charge neutrality tend to disfavor the 2SC phase [18, 19], it is found in phase diagrams calculated from NJL models, for example in Ref. [20] (see their Figs. 2 and 6) and in Ref. [21] (see their Fig. 7). In our calculations we shall neglect the effect of electric charge neutrality, so we treat the up and down

*Electronic address: alford@wuphys.wustl.edu

†Electronic address: aschmitt@wuphys.wustl.edu

quarks as having the same chemical potential and hence the same Fermi momentum. This has a quantitative effect, which we expect to be of order m_s^2/μ^2 , on the available phase space for the quark momenta. We therefore expect our results to deviate only slightly from the results for electrically neutral 2SC matter.

Bulk viscosity, as well as shear viscosity [22], is relevant to vibrational and rotational modes of a compact star, whose frequencies are typically in the kHz range [23]. In particular, for a rapidly rotating star there is the possibility of rotational “r-modes” that are unstable with respect to gravitational radiation [24–27]. This would lead to a drastic decrease of the rotation frequency of the star, which is incompatible with observations of rapidly rotating pulsars with periods of the order of ms. One mechanism to damp the instabilities is a nonzero viscosity of the fluid [28].

In general, bulk viscosity characterizes the response of the system to an externally imposed oscillating volume change. If the volume compression (and expansion) induces a change in the chemical composition of the matter, i.e., if it drives the system out of chemical equilibrium, then microscopic processes will try to re-equilibrate the system. If these processes occur on a timescale comparable to that of the driving oscillation then power dissipation will occur. Because the strange quark is massive, a volume oscillation causes a difference between the chemical potential of the s quark and that of the u and d quarks. The relevant microscopic re-equilibration process is the weak process $u + d \leftrightarrow u + s$ [29] which produces (annihilates) strangeness. (Leptonic processes are suppressed by their smaller phase space. However, we shall discuss the possibility that they might still yield a significant contribution to the bulk viscosity.) Strong processes can be neglected since they occur on much shorter time scales than the scale given by the oscillation of the star. This is in contrast to the context of heavy ion collisions where gluonic processes are important for the bulk viscosity [30]. Moreover, we do not consider a potential contribution from the Goldstone boson associated with the spontaneous breaking of $U(1)_A$ because this symmetry is explicitly broken at densities relevant for compact stars. Other (approximate) global symmetries are not broken in the 2SC phase, hence there are no other (pseudo) Goldstone bosons.

In order to compute the rate of the process $u + d \leftrightarrow u + s$ one has to consider the corresponding collision integral. In the case of a superconductor/superfluid this integral is considerably more complicated than in the unpaired phase. Some of the complication originates from the broken number conservation, allowing not only processes that consist of two ingoing and outgoing particles but also processes with three (four) particles coalescing into one (zero) particles and one (zero) particles decaying into three (four) particles. In these processes, particles are created from or deposited into the condensate. This effect is also present in more conventional superfluids such as ^3He [31]. Starting from the kinetic equation, we present a detailed derivation of the collision integral which contains all these possible processes.

An additional complication arises from the nature of the 2SC phase. The process $u_1 + d \leftrightarrow u_2 + s$ actually contains several subprocesses according to whether the incoming and outgoing states are gapped (up or down quarks that are red or green) or ungapped (all the other species). All these subprocesses are included naturally in our formal derivation. We encounter processes where zero, one, two, or three of the quarks u_1, d, u_2, s are gapped. Therefore, the 2SC phase is an interesting system to study the more general question of the quantitative effects of the energy gap for the rate of the microscopic process. We compute the rates for arbitrary temperatures T (up to the superconducting transition temperature), i.e., we go beyond the low-temperature regime, where the effect of the energy gap Δ is an exponential suppression of the rate.

A final subtlety is that the bulk viscosity is not a monotonic function of the rates of the equilibrating processes. The bulk viscosity is highest when those rates are closest to the time scale of the oscillation that is being damped. As we will see, this means that, depending what frequencies are physically relevant, a phase in which equilibration proceeds more slowly may have a higher bulk viscosity than one in which it proceeds quickly. Thus the 2SC phase, whose equilibration rate is always slower than that of unpaired quark matter, will turn out to have a larger bulk viscosity at kHz frequencies over a wide range of temperatures.

The paper is organized as follows. In Sec. II we define the bulk viscosity and point out an analogy to the power dissipation in an electric circuit with a capacitance and a resistance. The derivation of the rate of the process $u + d \leftrightarrow u + s$ in 2SC quark matter is presented in Sec. III. At the end of this section, in Sec. III E we discuss the physical content of the derived expression. In Sec. IV, the rate is evaluated in full generality and several limit cases (unpaired phase, zero-temperature limit) as well as several subprocesses and their contribution to the full result is discussed. We use these results to compute the bulk viscosity in Sec. V and conclude with Sec. VI.

II. DEFINITION OF BULK VISCOSITY

In this section we derive the expression for the bulk viscosity with respect to the process $u + s \leftrightarrow u + d$. This derivation is based on respective derivations of unpaired quark matter and variations of it for different microscopic processes [32–35]. We also point out an instructive analogy to an electric circuit with resistance and capacitance.

Before we do so, we notice that the following derivation includes several assumptions about other processes that potentially contribute to the bulk viscosity. First, there may be a contribution from the leptonic processes $u + e \leftrightarrow d + \nu$

and $u + e \leftrightarrow s + \nu$. In Appendix A we present a derivation of the bulk viscosity including these processes in addition to the nonleptonic process $u + s \leftrightarrow u + d$. The result (A13) is complicated compared to the result (21), derived in this section. Because of phase space restrictions, the leptonic processes can be expected to be slower than the non-leptonic one. However, as we discuss in Appendix A, their contribution can still be significant, depending on the external oscillation frequency. In this paper, we do not compute the rates of the leptonic processes microscopically. Therefore, we leave the study of their quantitative contribution to the bulk viscosity for future work.

Second, the derivation of the bulk viscosity below treats the effect of the process $u + s \leftrightarrow u + d$ solely through the flavor chemical potentials μ_u , μ_d , and μ_s , disregarding color degrees of freedom. This treatment is correct under the assumption of infinitely fast, color-changing strong processes as we show in Appendix B. In this appendix we set up a more general derivation of the bulk viscosity showing that in the absence of the strong interaction (or for not infinitely fast strong processes) the expression for the bulk viscosity is more complicated. For this aspect, see also discussion of the results of Fig. 7.

We start from the definition of the bulk viscosity [32–35]

$$\zeta \equiv 2 \left\langle \frac{dW}{dt} \right\rangle \left(\frac{V_0}{\delta V_0} \right)^2 \frac{1}{\omega^2}, \quad (1)$$

where we assume the volume of the system to oscillate with angular frequency ω and amplitude δV_0 about its equilibrium value V_0 ,

$$V(t) = V_0 + \delta V(t), \quad \delta V(t) = \delta V_0 \cos \omega t. \quad (2)$$

The average dissipated power per volume in one oscillation period $\tau \equiv 2\pi/\omega$ is

$$\left\langle \frac{dW}{dt} \right\rangle = -\frac{1}{\tau V_0} \int_0^\tau p(t) \frac{dV}{dt} dt, \quad (3)$$

where $p(t)$ is the pressure. We shall express the dissipated power in terms of $\delta V(t)$ and the resulting oscillation in $\delta\mu(t)$. Here, $\delta\mu$ is the difference between the s quark and the d quark chemical potential $\delta\mu = \mu_s - \mu_d$ which vanishes in chemical equilibrium. To this end, we write the pressure for small oscillations as

$$p(t) = p_0 + \left(\frac{\partial p}{\partial V} \right)_0 \delta V(t) + \left(\frac{\partial p}{\partial n_d} \right)_0 \delta n_d(t) + \left(\frac{\partial p}{\partial n_s} \right)_0 \delta n_s(t). \quad (4)$$

Here and in the following, the subscript 0 denotes equilibrium, i.e., $\delta\mu = \delta V = 0$, and n_s and n_d are the s - and d -quark number densities, respectively. We employ the thermodynamic relation

$$\left(\frac{\partial p}{\partial n_i} \right)_0 = -V_0 \left(\frac{\partial \mu_i}{\partial V} \right)_0, \quad i = d, s, \quad (5)$$

and use

$$-V_0 \left(\frac{\partial \mu_d}{\partial V} \right)_0 = \left(n_d \frac{\partial \mu_d}{\partial n_d} \right)_0 + \left(n_u \frac{\partial \mu_d}{\partial n_u} \right)_0, \quad (6a)$$

$$-V_0 \left(\frac{\partial \mu_s}{\partial V} \right)_0 = \left(n_s \frac{\partial \mu_s}{\partial n_s} \right)_0. \quad (6b)$$

Here we have taken into account that, in the 2SC phase, u and d quarks form Cooper pairs with each other. Therefore, μ_u and μ_d depend on *both* n_u and n_d . In contrast, μ_s solely depends on n_s because s quarks are unpaired. See Table I for the explicit form of the densities. Next, we express the change in densities in terms of the rate of the microscopic process, to be computed in Secs. III and IV,

$$\delta n_d(t) = -\delta n_s(t) = \int_0^t \Gamma_d[\delta\mu(t')] dt'. \quad (7)$$

Here, $\Gamma_d[\delta\mu(t)]$ is the number of d quarks per volume and time produced in the reaction $u + s \leftrightarrow u + d$. Since both directions of the reaction are taken into account, the rate is zero for $\delta\mu = 0$. In the present situation, however, a nonzero $\delta\mu$ is induced through the volume oscillation, rendering $\Gamma_d[\delta\mu(t)]$ nonzero. We shall use the linear approximation

$$\Gamma_d[\delta\mu(t)] = \lambda \delta\mu(t). \quad (8)$$

Inserting Eqs. (6) into (5), the result and (7) into Eq. (4), the result into Eq. (3), and making use of Eq. (8) we find

$$\left\langle \frac{dW}{dt} \right\rangle = -\frac{B}{V_0} \left\langle \left(\int_0^t \Gamma_d[\delta\mu(t')] dt' \right) \frac{dV}{dt} \right\rangle = B\lambda \langle \delta\mu(t) \delta v(t) \rangle, \quad (9)$$

where the right-hand side has been obtained via partial integration, we have abbreviated $\delta v(t) \equiv \delta V(t)/V_0$, and

$$B \equiv \left(n_u \frac{\partial \mu_d}{\partial n_u} \right)_0 + \left(n_d \frac{\partial \mu_d}{\partial n_d} \right)_0 - \left(n_s \frac{\partial \mu_s}{\partial n_s} \right)_0. \quad (10)$$

Finally, we have to connect the change in chemical potentials to the volume oscillation and the microscopic rate,

$$\frac{\partial \delta\mu}{\partial t} = \left(\frac{\partial \delta\mu}{\partial V} \right)_0 \frac{dV}{dt} + \left(\frac{\partial \delta\mu}{\partial n_d} \right)_0 \frac{dn_d}{dt} + \left(\frac{\partial \delta\mu}{\partial n_s} \right)_0 \frac{dn_s}{dt}, \quad (11)$$

where the change in densities is due to the microscopic process, $dn_d/dt = -dn_s/dt = \Gamma_d$. Consequently,

$$\frac{\partial \delta\mu}{\partial t} = B \frac{\partial \delta v}{\partial t} - \gamma \delta\mu(t), \quad (12)$$

where we abbreviated the characteristic (inverse) time scale set by the microscopic process by

$$\gamma \equiv C\lambda \quad (13)$$

where

$$C \equiv \left(\frac{\partial \mu_d}{\partial n_d} \right)_0 + \left(\frac{\partial \mu_s}{\partial n_s} \right)_0. \quad (14)$$

The equation for the power dissipation (9) in terms of the periodic external quantity $\delta v(t)$ and the response of the system $\delta\mu(t)$ together with the differential equation (12) for $\delta\mu(t)$ can be mapped exactly onto the analogous situation in an electric circuit. In this case, the external quantity is an alternating voltage $U(t)$ while the response of the system is the current $I(t)$. For a circuit with a resistance R , an inductance L and a capacitance C' , the corresponding equations are

$$\left\langle \frac{dW}{dt} \right\rangle = \langle I(t) U(t) \rangle, \quad (15a)$$

$$\dot{U}(t) = \dot{I}(t)R + L\ddot{I}(t) + \frac{I(t)}{C'}. \quad (15b)$$

Obviously, Eq. (15b) has the same form as Eq. (12) and we can identify “voltage”, “current”, “resistance”, “inductance”, and “capacitance” in the color superconductor,

$$U(t) \rightarrow \delta v(t), \quad I(t) \rightarrow \delta\mu(t), \quad R \rightarrow \frac{1}{B}, \quad L \rightarrow 0, \quad C' \rightarrow \frac{B}{\gamma}. \quad (16)$$

This analogy with an electric circuit is not only of a mathematical nature, we can also use it to understand the underlying physics. This is useful because the behavior of the bulk viscosity, unlike the shear viscosity, is somewhat counter-intuitive if one applies the daily life picture of a “viscous” fluid. Therefore, let us interpret the analogies in Eq. (16). First, the “resistance” of the system is proportional to $1/B$ with B given in Eq. (10). In particular, the resistance is infinite for vanishing B . This means that there is no response of the system to the external force, just as there is no current in a circuit with infinite resistance. The reason is that a vanishing B means that there is no difference of d and s flavor in the response to the change in density induced by the volume oscillations. Hence the system is still in chemical equilibrium and no energy is dissipated. A finite resistance occurs if there is a difference in the dispersion relations of d and s quarks, such as a different mass or different energy gaps. Only then does the system respond with an oscillating $\delta\mu(t)$ and both the power dissipation and the bulk viscosity are non-vanishing.

The “capacitance” is proportional to $1/\gamma$, where γ is the inverse time scale that characterizes the weak process. A slow process has a small γ , hence a large capacitance, meaning that the system can store a large amount of energy. This energy is only slowly released by producing d quarks (or s quarks, depending on the sign of $\delta\mu$) and thus re-approaching chemical equilibrium. This is just like a large capacitance which can store a large amount of electrical

charge. On the other hand, a fast process has a large γ and the capacitor can be discharged quickly (i.e. chemical equilibrium can be reached quickly).

Let us now continue with our derivation. We write the response of the system as

$$\delta\mu(t) = \text{Re}(\delta\mu_0 e^{i\omega t}) \quad (17)$$

with a complex amplitude $\delta\mu_0$. This expression is inserted into the differential equation (12). We obtain a phase lag ϕ of $\delta\mu(t)$ with respect to $\delta v(t)$,

$$\phi = \arctan \frac{\gamma}{\omega}. \quad (18)$$

The amplitude of the oscillation of the chemical potential is

$$|\delta\mu_0| = \frac{\delta V_0}{V_0} \frac{B\omega}{\sqrt{\gamma^2 + \omega^2}}, \quad (19)$$

and the power dissipation is

$$\left\langle \frac{dW}{dt} \right\rangle = \frac{1}{2} \frac{\delta V_0}{V_0} B \lambda \text{Re} \delta\mu_0 = \frac{1}{2} \left(\frac{\delta V_0}{V_0} \right)^2 \frac{B^2 \lambda \omega^2}{\gamma^2 + \omega^2}. \quad (20)$$

With the definition (1) we arrive at the following expression for the bulk viscosity,

$$\zeta = \frac{B^2}{C} \frac{\gamma}{\gamma^2 + \omega^2}, \quad (21)$$

This expression, together with the definitions (10), (13), and (14), is the main result of this section and shall be used in Sec. V.

In Table I, we show the explicit values for the coefficients B and C in unpaired and 2SC quark matter at zero temperature, derived from the quark densities as functions of the chemical potentials. The densities can be computed from the respective free energy in Ref. [18]. In order to obtain the partial derivatives appearing in B and C in the 2SC phase, one has to invert the Jacobian of the two-dimensional function $(n_u, n_d) = (n_u(\mu_u, \mu_d), n_d(\mu_u, \mu_d))$. We have neglected terms in higher orders of m_s and the pairing gap Δ . Moreover, we expect the difference in chemical potentials $\delta\nu \equiv (\mu_u - \mu_d)/2$ to be of the order of m_s^2/μ [18]. Therefore, we have also dropped higher order terms in $\delta\nu$. In the following calculation of the microscopic rate, we shall, for simplicity, consider the limit $\mu_u = \mu_d$. It is important to note that even in the limit $\Delta = 0$ the value of the coefficient C is different in the two considered phases. The reason is the “locking” of chemical potentials of the pairing fermions. In other words, gapped quasiparticles in the 2SC phase look as if their chemical potential (in the absence of pairing) was $\nu \equiv (\mu_u + \mu_d)/2$. This effect, the difference in C for unpaired and 2SC matter, is weakened by a nonzero temperature. We have checked numerically, however, that the difference remains sizable for all temperatures up to the transition temperature. Thus, for simplicity, we shall use the zero-temperature values from Table I as an approximation.

We have checked that electric neutrality has no sizable effect on the coefficients B and C . Requiring local electric neutrality at all times yields a constraint for the densities and chemical potentials via the condition $2n_u - n_d - n_s = 0$. Implementing this condition modifies the derivation for the bulk viscosity. However, to leading order the value of B^2/C turns out to be the same as in the non-neutral case.

III. DERIVATION OF THE RATE FOR THE PROCESS $u + s \leftrightarrow u + d$

In this section we derive the rate Γ_d , see Eq. (7), as a function of $\delta\mu$, i.e., for a system in chemical non-equilibrium. In equilibrium, $\delta\mu = 0$ and $\Gamma_d = 0$, since in this case the processes $u + s \rightarrow u + d$ and $u + d \rightarrow u + s$ have the same rate and thus the net rate Γ_d vanishes. We shall assume $\delta\mu = \mu_s - \mu_d > 0$, such that we expect a net production of d quarks, $\Gamma_d > 0$. The main result of this section is given by Eqs. (47), (50), and (51).

A. Formalism

We start from the kinetic equation which is derived from the Kadanoff-Baym equation [36] after applying a gradient expansion. For similar calculations within this formalism see Refs. [13, 14, 37, 38]. Close to equilibrium and employing

	unpaired	2SC
n_u	μ_u^3/π^2	$(\mu_u^3/3 + 2\nu^3/3 + \Delta^2\nu)/\pi^2$
n_d	μ_d^3/π^2	$(\mu_d^3/3 + 2\nu^3/3 + \Delta^2\nu)/\pi^2$
n_s	$\mu_s^3/\pi^2 [1 - 3m_s^2/(2\mu_s^2)]$	$\mu_s^3/\pi^2 [1 - 3m_s/(2\mu_s^2)]$
B	$m_s^2/(3\mu_d)$	$m_s^2/(3\mu_d) + 2\Delta^2/(9\nu)$
C	$2\pi^2/(3\mu_d^2) [1 + m_s^2/(4\mu_d^2)]$	$\pi^2/\mu_d^2 [1 + m_s^2/(6\mu_d^2) - \Delta^2/(18\mu_d^2) - 2\delta\nu/(3\mu_d)]$
B^2/C	$m_s^4/(6\pi^2)$	$m_s^4/(9\pi^2) + 4\Delta^2 m_s^2/(27\pi^2) + 4\Delta^4/(81\pi^2)$

TABLE I: Quark densities n_u , n_d , n_s and coefficients B and C for unpaired and 2SC quark matter for massless u and d quarks and a strange mass $m_s \ll \mu_u, \mu_d, \mu_s$. We have abbreviated $\nu \equiv (\mu_u + \mu_d)/2$ and $\delta\nu \equiv (\mu_u - \mu_d)/2$. The energy gap due to pairing of u and d quarks is denoted by Δ . For instance, the u quark density in the 2SC phase is given by three contributions: unpaired blue quarks yield a term $\mu_u^3/(3\pi^2)$; paired red and green quarks yield two terms, one contribution from a Fermi sphere filled up to the average chemical potential ν plus condensation energy proportional to Δ^2 . In the last line we give B^2/C to lowest order in m_s and Δ , which determines the maximum bulk viscosity.

the closed-time-path formalism we may use the kinetic equation

$$i \frac{\partial}{\partial t} \text{Tr}[\gamma_0 S^<(P_1)] = -\text{Tr}[S^>(P_1) \Sigma^<(P_1) - \Sigma^>(P_1) S^<(P_1)]. \quad (22)$$

Here and in the following, four-momenta are denoted by $P \equiv (p_0, \mathbf{p})$. The quantities $S^{<,>}$ and $\Sigma^{<,>}$ are the fermion propagators and self-energies, respectively. More precisely, they represent the d -quark propagator and the contribution to the d -quark self-energy originating from the (left) diagram shown in Fig. 1. Then, the left-hand side of Eq. (22), integrated over P_1 , basically is another way of writing Γ_d , while the right-hand side yields the collision integral for the process $u + s \leftrightarrow u + d$. Hence, in the following, we shall compute the rate Γ_d by evaluating the right-hand side of Eq. (22). To this end, we first define $S^{<,>}$ and $\Sigma^{<,>}$ for the 2SC phase (remainder of this subsection and Sec. III B) and then insert these definitions back into the right-hand side of Eq. (22) to obtain the collision integral (Secs. III C and III D).

Since we are describing a superconducting system, the fermion propagators are matrices in Nambu-Gorkov space,

$$S^{<,>}(P) = \begin{pmatrix} G_+^{<,>}(P) & F_-^{<,>}(P) \\ F_+^{<,>}(P) & G_-^{<,>}(P) \end{pmatrix}. \quad (23)$$

The explicit form of the “normal” and “anomalous” propagators $G_{\pm}^{<,>}$ and $F_{\pm}^{<,>}$ shall be given in the next subsection for the 2SC phase. The relevant part of the d -quark self-energy is given by the diagram in Fig. 1 (the right diagram in this figure is merely a reminder of our notation of the momenta),

$$\Sigma^{<,>}(P_1) = \frac{i}{M_W^4} \int \frac{d^4 P_4}{(2\pi)^4} \Gamma_{ud,-}^\mu S^{<,>}(P_4) \Gamma_{ud,+}^\nu \Pi_{\mu\nu}^{>,<}(P_1 - P_4), \quad (24)$$

where M_W is the W -boson mass and $\Gamma_{ud,\pm}^\mu$ is the vertex of the subprocess $d \leftrightarrow u + W^-$. The respective contribution to the W -boson polarization tensors are given by

$$\Pi_{\mu\nu}^{<,>}(Q) = -i \int \frac{d^4 P_2}{(2\pi)^4} \text{Tr}[\Gamma_{us,+}^\mu S^{>,<}(P_2 + Q) \Gamma_{us,-}^\nu S^{<,>}(P_2)], \quad (25)$$

where $\Gamma_{us,\pm}^\mu$ is the vertex of the subprocess $u + W^- \leftrightarrow s$. In Nambu-Gorkov space, the vertices are

$$\Gamma_{ud/us,\pm}^\mu = \frac{e V_{ud/us}}{2\sqrt{2} \sin \theta_W} \begin{pmatrix} \gamma^\mu (1 - \gamma^5) \tau_{ud/us,\pm} & 0 \\ 0 & -\gamma^\mu (1 + \gamma^5) \tau_{ud/us,\mp} \end{pmatrix}, \quad (26)$$

with the entries of the CKM matrix V_{ud} and V_{us} and the weak mixing angle θ_W , and

$$\tau_{ud,+} \equiv \begin{pmatrix} 0 & 1 & 0 \\ 0 & 0 & 0 \\ 0 & 0 & 0 \end{pmatrix}, \quad \tau_{ud,-} \equiv \begin{pmatrix} 0 & 0 & 0 \\ 1 & 0 & 0 \\ 0 & 0 & 0 \end{pmatrix}, \quad \tau_{us,+} \equiv \begin{pmatrix} 0 & 0 & 1 \\ 0 & 0 & 0 \\ 0 & 0 & 0 \end{pmatrix}, \quad \tau_{us,-} \equiv \begin{pmatrix} 0 & 0 & 0 \\ 0 & 0 & 0 \\ 1 & 0 & 0 \end{pmatrix} \quad (27)$$

are matrices in flavor space (with indices ordered u, d, s).

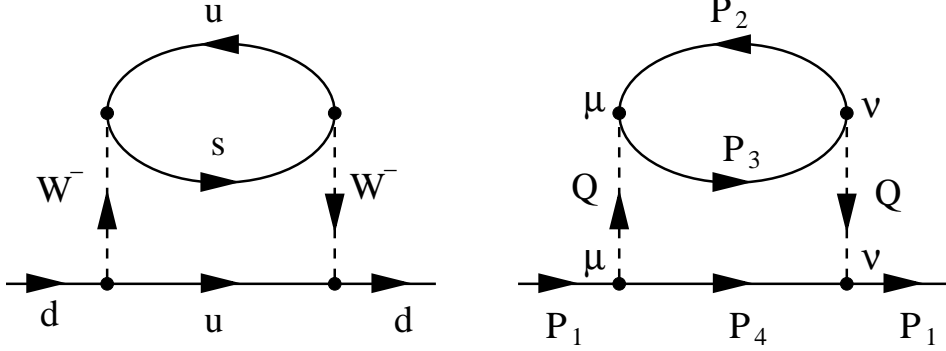


FIG. 1: Contribution to the d -quark self-energy, necessary to compute the rate for the process $u + s \leftrightarrow u + d$. The right diagram shows our notation of the corresponding momenta and Lorentz indices.

B. Quark propagators in the 2SC phase

We now specify the normal and anomalous propagators $G_{\pm}^{<,>}$ and $F_{\pm}^{<,>}$. We shall consider the simplest situation of massless quarks. In this case, the propagators in the 2SC phase are

$$G_{\pm}^{<,>}(K) = \sum_{r=1}^3 \mathcal{P}_r G_{\pm,r}^{<,>}(K) \gamma^0 \Lambda_{\mathbf{k}}^{\mp}, \quad F_{\pm}^{<,>}(K) = J_3 I_3 F_{\pm,1}^{<,>}(K) \gamma^5 \Lambda_{\mathbf{k}}^{\mp}. \quad (28)$$

The index r labels the different quasiparticle excitations, which are explained below and shown in Table II. The quantities $\Lambda_{\mathbf{k}}^{\mp} \equiv (1 \mp \gamma^0 \gamma \cdot \hat{\mathbf{k}})/2$, with $\hat{\mathbf{k}} \equiv \mathbf{k}/k$, are energy projectors, $(I_i)_{jk} = (J_i)_{jk} = -i\epsilon_{ijk}$ ($i, j, k \leq 1, 2, 3$) are matrices in flavor and color space, respectively, and

$$G_{\pm,r}^{>}(K) \equiv -2\pi i \left\{ B_{k,r}^{\pm} f(\varepsilon_{k,r}) \delta(k_0 \pm \mu_r - \varepsilon_{k,r}) + B_{k,r}^{\mp} [1 - f(\varepsilon_{k,r})] \delta(k_0 \pm \mu_r + \varepsilon_{k,r}) \right\}, \quad (29a)$$

$$G_{\pm,r}^{<}(K) \equiv -2\pi i \left\{ B_{k,r}^{\pm} [1 - f(\varepsilon_{k,r})] \delta(k_0 \pm \mu_r - \varepsilon_{k,r}) + B_{k,r}^{\mp} f(\varepsilon_{k,r}) \delta(k_0 \pm \mu_r + \varepsilon_{k,r}) \right\}, \quad (29b)$$

$$F_{\pm,r}^{>}(K) \equiv 2\pi i \frac{\Delta}{2\varepsilon_{k,r}} \left\{ f(\varepsilon_{k,r}) \delta(k_0 \mp \mu_r - \varepsilon_{k,r}) - [1 - f(\varepsilon_{k,r})] \delta(k_0 \mp \mu_r + \varepsilon_{k,r}) \right\}, \quad (29c)$$

$$F_{\pm,r}^{<}(K) \equiv 2\pi i \frac{\Delta}{2\varepsilon_{k,r}} \left\{ [1 - f(\varepsilon_{k,r})] \delta(k_0 \pm \mu_r - \varepsilon_{k,r}) - f(\varepsilon_{k,r}) \delta(k_0 \pm \mu_r + \varepsilon_{k,r}) \right\}. \quad (29d)$$

Here, we have introduced the Bogoliubov coefficients

$$B_{k,r}^{\pm} \equiv \frac{\varepsilon_{k,r} \pm (\mu_r - k)}{2\varepsilon_{k,r}}. \quad (30)$$

Moreover, f is the fermion distribution function. For the right-hand side of the kinetic equation, we shall approximate f by its equilibrium form,

$$f(\varepsilon) \equiv \frac{1}{e^{\varepsilon/T} + 1}. \quad (31)$$

We have neglected the antiparticle contribution to the propagators. For simplicity, we assume $\mu_u = \mu_d \equiv \mu$. This is somewhat unrealistic since it violates overall electric charge neutrality. However, a more realistic scenario $\mu_u \neq \mu_d$ would lead to some additional (notational) complication and does not alter our results qualitatively. With this simplification, we have 3 different quasiparticle dispersion relations, $\varepsilon_{k,r}$, with $r = 1, 2, 3$. They are shown in Table II with Δ being the energy gap induced by Cooper pairing of u and d quarks. The condensate picks a certain direction in color and flavor space, here J_3 and I_3 , respectively, leaving one color of u and d quarks as well as all s quarks unpaired. Formally, each of the three modes lives in a subspace of the 9-dimensional color-flavor space, which is given by the corresponding projectors \mathcal{P}_i occurring in the normal propagators $G_{\pm}^{<,>}(K)$. The projectors are shown in the last column of Table II. The dimensions of the subspaces are 4, 2, 3, respectively. In the anomalous propagators, only the gapped modes, $r = 1$, contribute.

r	quarks	dispersion	projector
1	ru, rd, gu, gd	$\varepsilon_{k,1} = \sqrt{(k - \mu)^2 + \Delta^2}$	$\mathcal{P}_1 = I_3^2 J_3^2$
2	bu, bd	$\varepsilon_{k,2} = k - \mu $	$\mathcal{P}_2 = I_3^2 (1 - J_3^2)$
3	rs, gs, bs	$\varepsilon_{k,3} = k - \mu_s $	$\mathcal{P}_3 = 1 - I_3^2$

TABLE II: Quasiparticle modes in the 2SC phase for ultra-relativistic quarks and $\mu_u = \mu_d \equiv \mu$.

C. W -boson polarization tensor

Next, we compute the contribution to the W -boson polarization tensor that occurs in the d -quark self-energy, Eq. (24). From its definition (25) we obtain after inserting Eq. (23) and performing the trace over Nambu-Gorkov space

$$\begin{aligned} \Pi_{\mu\nu}^{<,>}(Q) = & -i \frac{e^2 V_{us}^2}{8 \sin^2 \theta_W} \int \frac{d^4 P_2}{(2\pi)^4} \left\{ \text{Tr}[\gamma^\mu (1 - \gamma^5) \tau_{us,+} G_+^{>,<} (P_2 + Q) \gamma^\nu (1 - \gamma^5) \tau_{us,-} G_+^{<,>} (P_2)] \right. \\ & + \text{Tr}[\gamma^\mu (1 + \gamma^5) \tau_{us,-} G_-^{>,<} (P_2 + Q) \gamma^\nu (1 + \gamma^5) \tau_{us,+} G_-^{<,>} (P_2)] \\ & - \text{Tr}[\gamma^\mu (1 - \gamma^5) \tau_{us,+} F_-^{>,<} (P_2 + Q) \gamma^\nu (1 + \gamma^5) \tau_{us,+} F_+^{<,>} (P_2)] \\ & \left. - \text{Tr}[\gamma^\mu (1 + \gamma^5) \tau_{us,-} F_+^{>,<} (P_2 + Q) \gamma^\nu (1 - \gamma^5) \tau_{us,-} F_-^{<,>} (P_2)] \right\}. \end{aligned} \quad (32)$$

We assume without explicit proof that the second (fourth) term yields the same contribution as the first (third) term because this is just the charge-conjugate counterpart. Next we use Eq. (28) and perform the trace over color and flavor space. We make use of

$$\tau_{us,+} \mathcal{P}_1 = 0, \quad \tau_{us,-} \mathcal{P}_1 = \tau_{us,-} J_3^2, \quad (33a)$$

$$\tau_{us,+} \mathcal{P}_2 = 0, \quad \tau_{us,-} \mathcal{P}_2 = \tau_{us,-} (1 - J_3^2), \quad (33b)$$

$$\tau_{us,+} \mathcal{P}_3 = \tau_{us,+}, \quad \tau_{us,-} \mathcal{P}_3 = 0, \quad (33c)$$

$$\tau_{us,\pm} I_3 \tau_{us,\pm} I_3 = 0. \quad (33d)$$

Because of Eq. (33d), the anomalous propagators yield no contribution. Then, with $P_3 = P_2 + Q$ and denoting

$$\mathcal{T}^{\mu\nu}(\hat{\mathbf{p}}, \hat{\mathbf{k}}) \equiv \text{Tr}[\gamma^\mu (1 - \gamma^5) \gamma^0 \Lambda_{\mathbf{p}}^- \gamma^\nu (1 - \gamma^5) \gamma^0 \Lambda_{\mathbf{k}}^-], \quad (34)$$

we obtain

$$\Pi_{\mu\nu}^{<,>}(Q) = -2i \frac{e^2 V_{us}^2}{8 \sin^2 \theta_W} \int \frac{d^4 P_2}{(2\pi)^4} \mathcal{T}^{\mu\nu}(\hat{\mathbf{p}}_3, \hat{\mathbf{p}}_2) [2G_{+,3}^{>,<} (P_3) G_{+,1}^{<,>} (P_2) + G_{+,3}^{>,<} (P_3) G_{+,2}^{<,>} (P_2)]. \quad (35)$$

Inserting the propagators from Eqs. (29) into this expression and using $1 - f(\varepsilon) = f(-\varepsilon)$ for the equilibrium function (31) yields

$$\begin{aligned} \Pi_{\mu\nu}^{<,>}(Q) = & 4\pi i \frac{e^2 V_{us}^2}{8 \sin^2 \theta_W} \sum_{e_2 e_3} \int \frac{d^3 \mathbf{p}_2}{(2\pi)^3} \mathcal{T}^{\mu\nu}(\hat{\mathbf{p}}_3, \hat{\mathbf{p}}_2) \\ & \times \left\{ 2B_{p_3,3}^{e_3} B_{p_2,1}^{e_2} f(\pm e_3 \varepsilon_{p_3,3}) f(\mp e_2 \varepsilon_{p_2,1}) \delta(q_0 - e_3 \varepsilon_{p_3,3} + e_2 \varepsilon_{p_2,1} + \delta\mu) \right. \\ & \left. + B_{p_3,3}^{e_3} B_{p_2,2}^{e_2} f(\pm e_3 \varepsilon_{p_3,3}) f(\mp e_2 \varepsilon_{p_2,2}) \delta(q_0 - e_3 \varepsilon_{p_3,3} + e_2 \varepsilon_{p_2,2} + \delta\mu) \right\}, \end{aligned} \quad (36)$$

where the sum runs over $e_2, e_3 = \pm 1$, and the upper (lower) sign corresponds to $\Pi^<$ ($\Pi^>$). Remember that the quark loop in the polarization tensor contains a u and an s quark. Therefore, both contributions in curly brackets contain the third mode, $r = 3$, describing an (ungapped) s quark. For the u quark, there are two options. The first term in curly brackets describes a gapped u quark, $r = 1$. The factor 2 in front of this term originates from color degeneracy: Both red and green u quarks are gapped. The second term in curly brackets describes an ungapped blue u quark.

D. Collision integral

Upon inserting Eq. (24) into Eq. (22), the kinetic equation becomes

$$i \frac{\partial}{\partial t} \text{Tr}[\gamma_0 S^<(P_1)] = - \frac{i}{M_W^4} \int \frac{dP_4}{(2\pi)^4} \text{Tr}[S^>(P_1) \Gamma_{ud,-}^\mu S^<(P_4) \Gamma_{ud,+}^\nu \Pi_{\mu\nu}^>(P_1 - P_4) - \Gamma_{ud,-}^\mu S^>(P_4) \Gamma_{ud,+}^\nu S^<(P_1) \Pi_{\mu\nu}^<(P_1 - P_4)]. \quad (37)$$

Hence, in order to evaluate the right-hand side of this equation, we need the traces

$$\begin{aligned} \text{Tr}[S^>(P_1) \Gamma_{ud,-}^\mu S^<(P_4) \Gamma_{ud,+}^\nu] &= \frac{e^2 V_{ud}^2}{8 \sin^2 \theta_W} \left\{ \text{Tr}[G_+^>(P_1) \gamma^\mu (1 - \gamma^5) \tau_{ud,-} G_+^<(P_4) \gamma^\nu (1 - \gamma^5) \tau_{ud,+}] \right. \\ &\quad + \text{Tr}[G_-^>(P_1) \gamma^\mu (1 + \gamma^5) \tau_{ud,+} G_-^<(P_4) \gamma^\nu (1 + \gamma^5) \tau_{ud,-}] \\ &\quad - \text{Tr}[F_-^>(P_1) \gamma^\mu (1 + \gamma^5) \tau_{ud,+} F_+^<(P_4) \gamma^\nu (1 - \gamma^5) \tau_{ud,+}] \\ &\quad \left. - \text{Tr}[F_+^>(P_1) \gamma^\mu (1 - \gamma^5) \tau_{ud,-} F_-^<(P_4) \gamma^\nu (1 + \gamma^5) \tau_{ud,-}] \right\}, \end{aligned} \quad (38)$$

and

$$\begin{aligned} \text{Tr}[\Gamma_{ud,-}^\mu S^>(P_4) \Gamma_{ud,+}^\nu S^<(P_1)] &= \frac{e^2 V_{ud}^2}{8 \sin^2 \theta_W} \left\{ \text{Tr}[\gamma^\mu (1 - \gamma^5) \tau_{ud,-} G_+^>(P_4) \gamma^\nu (1 - \gamma^5) \tau_{ud,+} G_+^<(P_1)] \right. \\ &\quad + \text{Tr}[\gamma^\mu (1 + \gamma^5) \tau_{ud,+} G_-^>(P_4) \gamma^\nu (1 + \gamma^5) \tau_{ud,-} G_-^<(P_1)] \\ &\quad - \text{Tr}[\gamma^\mu (1 - \gamma^5) \tau_{ud,-} F_-^>(P_4) \gamma^\nu (1 + \gamma^5) \tau_{ud,-} F_+^<(P_1)] \\ &\quad \left. - \text{Tr}[\gamma^\mu (1 + \gamma^5) \tau_{ud,+} F_+^>(P_4) \gamma^\nu (1 - \gamma^5) \tau_{ud,+} F_-^<(P_1)] \right\}. \end{aligned} \quad (39)$$

Again, in both expressions, the first (third) and second (fourth) traces yield identical contributions. For the traces over color and flavor space we make use of

$$\tau_{ud,\pm} \mathcal{P}_1 = \tau_{ud,\pm} J_3^2, \quad (40a)$$

$$\tau_{ud,\pm} \mathcal{P}_2 = \tau_{ud,\pm} (1 - J_3^2), \quad (40b)$$

$$\tau_{ud,\pm} \mathcal{P}_3 = 0, \quad (40c)$$

$$\tau_{ud,+} I_3 \tau_{ud,+} I_3 = I_1^2 - 1 \quad (40d)$$

$$\tau_{ud,-} I_3 \tau_{ud,-} I_3 = I_2^2 - 1. \quad (40e)$$

This shows that, in contrast to the W -boson polarization tensor, the traces containing anomalous propagators do not vanish. We obtain

$$\begin{aligned} \text{Tr}[S^>(P_1) \Sigma^<(P_1)] &= i \frac{e^2 V_{ud}^2}{4 M_W^4 \sin^2 \theta_W} \int \frac{d^4 P_4}{(2\pi)^4} \left\{ [2G_{+,1}^>(P_1) G_{+,1}^<(P_4) + G_{+,2}^>(P_1) G_{+,2}^<(P_4)] \mathcal{T}^{\mu\nu}(\hat{\mathbf{p}}_4, \hat{\mathbf{p}}_1) \right. \\ &\quad \left. + 2F_{-,1}^>(P_1) F_{+,1}^<(P_4) \mathcal{U}^{\mu\nu}(\hat{\mathbf{p}}_1, \hat{\mathbf{p}}_4) \right\} \Pi_{\mu\nu}^>(P_1 - P_4), \end{aligned} \quad (41)$$

and

$$\begin{aligned} \text{Tr}[\Sigma^>(P_1) S^<(P_1)] &= i \frac{e^2 V_{ud}^2}{4 M_W^4 \sin^2 \theta_W} \int \frac{d^4 P_4}{(2\pi)^4} \left\{ [2G_{+,1}^>(P_4) G_{+,1}^<(P_1) + G_{+,2}^>(P_4) G_{+,2}^<(P_1)] \mathcal{T}^{\mu\nu}(\hat{\mathbf{p}}_4, \hat{\mathbf{p}}_1) \right. \\ &\quad \left. + 2F_{-,1}^>(P_4) F_{+,1}^<(P_1) \mathcal{U}^{\mu\nu}(\hat{\mathbf{p}}_4, \hat{\mathbf{p}}_1) \right\} \Pi_{\mu\nu}^<(P_1 - P_4), \end{aligned} \quad (42)$$

where we defined the trace over Dirac space,

$$\mathcal{U}^{\mu\nu}(\hat{\mathbf{p}}, \hat{\mathbf{k}}) \equiv \text{Tr}[\gamma^\mu (1 - \gamma^5) \gamma^5 \Lambda_{\mathbf{p}}^+ \gamma^\nu (1 + \gamma^5) \gamma^5 \Lambda_{\mathbf{k}}^-]. \quad (43)$$

Again, the different contributions in curly brackets in Eqs. (41) and (42) are easy to understand. Remember that these expressions describe the subprocess $d \leftrightarrow W^- + u$. Therefore, one contribution comes from the gapped u and d quarks, $r = 1$. This mode also yields a contribution from the anomalous propagators. It describes red and green quarks, hence the prefactor 2. The second contribution comes from the ungapped mode, $r = 2$, which describes blue

quarks and which, of course, yields no anomalous contribution. Due to color conservation of the weak interaction, no mixing of the two modes is possible.

Next, we perform the integration over p_{40} . Moreover, we shall integrate the kinetic equation over d -quark energies p_{10} and momenta \mathbf{p}_1 , because we are interested in the total rate, not in the rate as a function of momentum. Therefore, we need the results (derived by inserting the propagators from Eqs. (29) into Eqs. (41) and (42))

$$\int_{-\infty}^{\infty} \frac{dp_{10}}{2\pi} \text{Tr}[S^>(P_1)\Sigma^<(P_1)] = -i \frac{e^2 V_{ud}^2}{4M_W^4 \sin^2 \theta_W} \sum_{e_1 e_4} \int \frac{d^3 \mathbf{p}_4}{(2\pi)^3} \left\{ 2 \left[B_{p_1,1}^{e_1} B_{p_4,1}^{e_4} \mathcal{T}^{\mu\nu}(\hat{\mathbf{p}}_4, \hat{\mathbf{p}}_1) + \frac{e_1 e_4 \Delta^2}{4\varepsilon_{p_1,1} \varepsilon_{p_4,1}} \mathcal{U}^{\mu\nu}(\hat{\mathbf{p}}_1, \hat{\mathbf{p}}_4) \right] \right. \\ \times f(e_1 \varepsilon_{p_1,1}) f(-e_4 \varepsilon_{p_4,1}) \Pi_{\mu\nu}^>(e_1 \varepsilon_{p_1,1} - e_4 \varepsilon_{p_4,1}, \mathbf{p}_1 - \mathbf{p}_4) \\ \left. + B_{p_1,2}^{e_1} B_{p_4,2}^{e_4} \mathcal{T}^{\mu\nu}(\hat{\mathbf{p}}_4, \hat{\mathbf{p}}_1) f(e_1 \varepsilon_{p_1,2}) f(-e_4 \varepsilon_{p_4,2}) \Pi_{\mu\nu}^>(e_1 \varepsilon_{p_1,2} - e_4 \varepsilon_{p_4,2}, \mathbf{p}_1 - \mathbf{p}_4) \right\}, \quad (44)$$

and

$$\int_{-\infty}^{\infty} \frac{dp_{10}}{2\pi} \text{Tr}[\Sigma^>(P_1)S^<(P_1)] = -i \frac{e^2 V_{ud}^2}{4M_W^4 \sin^2 \theta_W} \sum_{e_1 e_4} \int \frac{d^3 \mathbf{p}_4}{(2\pi)^3} \left\{ 2 \left[B_{p_1,1}^{e_1} B_{p_4,1}^{e_4} \mathcal{T}^{\mu\nu}(\hat{\mathbf{p}}_4, \hat{\mathbf{p}}_1) + \frac{e_1 e_4 \Delta^2}{4\varepsilon_{p_1,1} \varepsilon_{p_4,1}} \mathcal{U}^{\mu\nu}(\hat{\mathbf{p}}_4, \hat{\mathbf{p}}_1) \right] \right. \\ \times f(-e_1 \varepsilon_{p_1,1}) f(e_4 \varepsilon_{p_4,1}) \Pi_{\mu\nu}^<(e_1 \varepsilon_{p_1,1} - e_4 \varepsilon_{p_4,1}, \mathbf{p}_1 - \mathbf{p}_4) \\ \left. + B_{p_1,2}^{e_1} B_{p_4,2}^{e_4} \mathcal{T}^{\mu\nu}(\hat{\mathbf{p}}_4, \hat{\mathbf{p}}_1) f(-e_1 \varepsilon_{p_1,2}) f(e_4 \varepsilon_{p_4,2}) \Pi_{\mu\nu}^<(e_1 \varepsilon_{p_1,2} - e_4 \varepsilon_{p_4,2}, \mathbf{p}_1 - \mathbf{p}_4) \right\}. \quad (45)$$

Then, in order to obtain the right-hand side of Eq. (22) (integrated over P_1), we have to insert Eq. (36) into Eqs. (44) and (45) and the result into Eq. (22). One needs the explicit results for the Dirac traces and contractions of the form $\mathcal{T}^{\mu\nu} \mathcal{T}_{\mu\nu}$ and $\mathcal{U}^{\mu\nu} \mathcal{T}_{\mu\nu}$. They are given in Appendix C. As shown in this appendix, the contractions of the form $\mathcal{U}^{\mu\nu} \mathcal{T}_{\mu\nu}$, i.e., the ones originating from the contribution of anomalous propagators, are complex. However, after the angular integration in the collision integral, the imaginary parts vanish, see Appendix D 2. Therefore, we shall continue with only the real parts of these contractions.

The left-hand side of the kinetic equation has also to be integrated over P_1 . Furthermore, we have to project onto the d -flavor subspace. This is done by inserting the projector $\mathcal{Q}_d \equiv \text{diag}(0, 1, 0)$. We obtain

$$i \frac{\partial}{\partial t} \int \frac{dP_1}{(2\pi)^4} \text{Tr}[\gamma_0 \mathcal{Q}_d S^<(P_1)] = -4 \frac{\partial}{\partial t} \int \frac{d^3 \mathbf{p}_1}{(2\pi)^3} \left\{ 2B_{p_1,1}^+ f(\varepsilon_{p_1,1}) + 2B_{p_1,1}^- [1 - f(\varepsilon_{p_1,1})] \right. \\ \left. + B_{p_1,2}^+ f(\varepsilon_{p_1,2}) + B_{p_1,2}^- [1 - f(\varepsilon_{p_1,2})] \right\} \\ \equiv -4 \frac{\partial}{\partial t} \int \frac{d^3 \mathbf{p}_1}{(2\pi)^3} f_d(t, \mathbf{p}_1) \equiv -4\Gamma_d, \quad (46)$$

where $f_d(t, \mathbf{p}_1)$ is the (non-equilibrium) d -flavor distribution function. Hence, the rate Γ_d is the change of the total number of d quarks per time and volume. This is the microscopic definition of Γ_d which implicitly has been used in Sec. II. The factor 4 arises after performing the trace; it originates from the Nambu-Gorkov doubling and spin degeneracy. Putting the results for the left-hand and right-hand sides together and dividing both sides by 4 yields

$$\Gamma_d = 4\Gamma_d^{1131} + 2\Gamma_d^{1231} + 2\Gamma_d^{2132} + \Gamma_d^{2232} + 4\tilde{\Gamma}_d^{1131} + 2\tilde{\Gamma}_d^{1231}. \quad (47)$$

We shall explain the physical meaning of the several terms in the next subsection. Their explicit form is

$$\Gamma_d^{r_1 r_2 r_3 r_4} \equiv 128\pi^4 G_F^2 V_{ud}^2 V_{us}^2 \sum_{e_1 e_2 e_3 e_4} \int \frac{d^3 \mathbf{p}_1}{(2\pi)^3} \int \frac{d^3 \mathbf{p}_2}{(2\pi)^3} \int \frac{d^3 \mathbf{p}_3}{(2\pi)^3} \int \frac{d^3 \mathbf{p}_4}{(2\pi)^3} \delta(\mathbf{p}_1 + \mathbf{p}_2 - \mathbf{p}_3 - \mathbf{p}_4) \\ \times (1 - \hat{\mathbf{p}}_1 \cdot \hat{\mathbf{p}}_2)(1 - \hat{\mathbf{p}}_3 \cdot \hat{\mathbf{p}}_4) B_1^{e_1} B_2^{e_2} B_3^{e_3} B_4^{e_4} \delta(e_1 \varepsilon_1 + e_2 \varepsilon_2 - e_3 \varepsilon_3 - e_4 \varepsilon_4 + \delta\mu) \\ \times [f(e_1 \varepsilon_1) f(e_2 \varepsilon_2) f(-e_3 \varepsilon_3) f(-e_4 \varepsilon_4) - f(-e_1 \varepsilon_1) f(-e_2 \varepsilon_2) f(e_3 \varepsilon_3) f(e_4 \varepsilon_4)], \quad (48)$$

and

$$\tilde{\Gamma}_d^{r_1 r_2 r_3 r_4} \equiv 64\pi^4 G_F^2 V_{ud}^2 V_{us}^2 \sum_{e_1 e_2 e_3 e_4} \int \frac{d^3 \mathbf{p}_1}{(2\pi)^3} \int \frac{d^3 \mathbf{p}_2}{(2\pi)^3} \int \frac{d^3 \mathbf{p}_3}{(2\pi)^3} \int \frac{d^3 \mathbf{p}_4}{(2\pi)^3} \delta(\mathbf{p}_1 + \mathbf{p}_2 - \mathbf{p}_3 - \mathbf{p}_4) \\ \times [(1 - \hat{\mathbf{p}}_4 \cdot \hat{\mathbf{p}}_3)(1 - \hat{\mathbf{p}}_1 \cdot \hat{\mathbf{p}}_2) + (1 + \hat{\mathbf{p}}_1 \cdot \hat{\mathbf{p}}_3)(1 + \hat{\mathbf{p}}_4 \cdot \hat{\mathbf{p}}_2) - (1 + \hat{\mathbf{p}}_1 \cdot \hat{\mathbf{p}}_4)(1 + \hat{\mathbf{p}}_3 \cdot \hat{\mathbf{p}}_2)] \\ \times \frac{e_1 \Delta}{2\varepsilon_1} B_2^{e_2} B_3^{e_3} \frac{e_4 \Delta}{2\varepsilon_4} \delta(e_1 \varepsilon_1 + e_2 \varepsilon_2 - e_3 \varepsilon_3 - e_4 \varepsilon_4 + \delta\mu) \\ \times [f(e_1 \varepsilon_1) f(e_2 \varepsilon_2) f(-e_3 \varepsilon_3) f(-e_4 \varepsilon_4) - f(-e_1 \varepsilon_1) f(-e_2 \varepsilon_2) f(e_3 \varepsilon_3) f(e_4 \varepsilon_4)], \quad (49)$$

with the Fermi coupling constant G_F . We have introduced an additional integration over \mathbf{p}_3 and the corresponding δ -function for momentum conservation. This was implicitly present in the previous expressions. Moreover, we have abbreviated the quasiparticle energies with momentum p_i and excitation branch r_i by $\varepsilon_i \equiv \varepsilon_{p_i, r_i}$ and the Bogoliubov coefficients by $B_i^{e_i} \equiv B_{p_i, r_i}^{e_i}$. We may now perform the angular integration. This calculation is identical to the unpaired phase [39], see Appendix D. The results are

$$\Gamma_d^{r_1 r_2 r_3 r_4} \equiv \frac{G_F^2 V_{ud}^2 V_{us}^2}{8\pi^5} \sum_{e_1 e_2 e_3 e_4} \int_{p_1 p_2 p_3 p_4} I(p_1, p_2, p_3, p_4) B_1^{e_1} B_2^{e_2} B_3^{e_3} B_4^{e_4} \delta(e_1 \varepsilon_1 + e_2 \varepsilon_2 - e_3 \varepsilon_3 - e_4 \varepsilon_4 + \delta\mu) \times [f(e_1 \varepsilon_1) f(e_2 \varepsilon_2) f(-e_3 \varepsilon_3) f(-e_4 \varepsilon_4) - f(-e_1 \varepsilon_1) f(-e_2 \varepsilon_2) f(e_3 \varepsilon_3) f(e_4 \varepsilon_4)] , \quad (50)$$

and

$$\tilde{\Gamma}_d^{r_1 r_2 r_3 r_4} \equiv \frac{G_F^2 V_{ud}^2 V_{us}^2}{16\pi^5} \sum_{e_1 e_2 e_3 e_4} \int_{p_1 p_2 p_3 p_4} \tilde{I}(p_1, p_2, p_3, p_4) \frac{e_1 \Delta}{2\varepsilon_1} B_2^{e_2} B_3^{e_3} \frac{e_4 \Delta}{2\varepsilon_4} \delta(e_1 \varepsilon_1 + e_2 \varepsilon_2 - e_3 \varepsilon_3 - e_4 \varepsilon_4 + \delta\mu) \times [f(e_1 \varepsilon_1) f(e_2 \varepsilon_2) f(-e_3 \varepsilon_3) f(-e_4 \varepsilon_4) - f(-e_1 \varepsilon_1) f(-e_2 \varepsilon_2) f(e_3 \varepsilon_3) f(e_4 \varepsilon_4)] , \quad (51)$$

where the functions I and \tilde{I} are given in Eqs. (D13) and where we abbreviated

$$\int_{p_1 p_2 p_3 p_4} \equiv \int_0^\infty dp_1 \int_0^\infty dp_2 \int_0^\infty dp_3 \int_0^\infty dp_4 . \quad (52)$$

E. Subprocesses and unpaired phase limit

The collision integral is the sum of six terms, see Eq. (47), which are shown diagrammatically in Fig. 2 (in the same order as they appear in the equation). The superscripts at Γ_d and $\tilde{\Gamma}_d$ in Eq. (47) correspond to the momenta in the order p_1, p_2, p_3, p_4 , i.e., they describe the particles d, u_1, s, u_2 , respectively, see diagrams in Fig. 1. The combinatorics of the process is constrained by color conservation for the vertices $d \leftrightarrow u_2 + W^-$ and $u_1 + W^- \leftrightarrow s$. Consequently, d and u_2 as well as s and u_1 must have the same color. Hence, from Table II we conclude that d and u_2 must be either both gapped ($r = 1$) or both ungapped ($r = 2$). This can be seen in Fig. 2, where we have added the gap Δ at the fermion line whenever the corresponding mode is gapped. It can also be seen in Eq. (47), where the pair of first and last superscripts is either (1,1) or (2,2). Furthermore, the second and third superscript can be (1,3) or (2,3), describing a (red or green) gapped u and a (red or green) s or a (blue) ungapped u and a (blue) s , respectively. The s quark is ungapped for all colors. Combining these pairs and counting color degeneracies yields the six terms with respective prefactors in Eq. (47) and Fig. 2. In the cases where both d and u_2 are gapped, there is an additional contribution from the anomalous propagators. This is denoted by $\tilde{\Gamma}_d$ in Eq. (47) and by a condensate insertion in Fig. 2. From the diagrams it is clear that there can be no condensate insertion for u_1 . This would lead to a violation of electric charge conservation at the vertex $u_1 + W^- \leftrightarrow s$. Summarizing the result of the combinatorics, we have found that the process $d + u_1 \leftrightarrow s + u_2$ in the 2SC phase can be considered as composed of several subprocesses, where zero, one, two, or three of the participating particles have a gap in their excitation spectrum.

From Eqs. (50) and (51) we see that the process $d + u_1 \leftrightarrow s + u_2$ not only contains several subprocesses due to the 2SC pairing pattern, also every single of these subprocesses is written as a sum over 16 terms, expressed as a sum over e_1, \dots, e_4 . To understand the physical meaning of this sum, it is instructive to rewrite it and recover the unpaired phase limit. The change of variables described in the following is illustrated in Fig. 3. We may rewrite every single sum over e_i by observing that for any function F we have

$$\sum_{e_i} \int_0^\infty dp_i B_i^{e_i} F(e_i \varepsilon_i) = \sum_{e_i} \int_0^\infty dp_i \tilde{B}_i^{e_i} F(-e_i \tilde{\varepsilon}_i) , \quad (53)$$

where the new Bogoliubov coefficients and quasiparticle energies are defined as

$$\tilde{B}_i^{e_i} \equiv \frac{1}{2} \left(1 + e_i \frac{p_i - \mu_i}{\tilde{\varepsilon}_i} \right) , \quad \tilde{\varepsilon}_i \equiv \text{sgn}(p_i - \mu_i) \varepsilon_i . \quad (54)$$

Consequently, in Eqs. (50) and (51) we can replace $B_i^{e_i}$ by $\tilde{B}_i^{e_i}$ and $e_i \varepsilon_i$ by $-e_i \tilde{\varepsilon}_i$. Then, we obtain for the contribution from the normal propagators,

$$\Gamma_d^{r_1 r_2 r_3 r_4} \equiv \frac{G_F^2 V_{ud}^2 V_{us}^2}{8\pi^5} \sum_{e_1 e_2 e_3 e_4} \int_{p_1 p_2 p_3 p_4} I(p_1, p_2, p_3, p_4) \tilde{B}_1^{e_1} \tilde{B}_2^{e_2} \tilde{B}_3^{e_3} \tilde{B}_4^{e_4} \delta(e_1 \tilde{\varepsilon}_1 + e_2 \tilde{\varepsilon}_2 - e_3 \tilde{\varepsilon}_3 - e_4 \tilde{\varepsilon}_4 - \delta\mu) \times [f(-e_1 \tilde{\varepsilon}_1) f(-e_2 \tilde{\varepsilon}_2) f(e_3 \tilde{\varepsilon}_3) f(e_4 \tilde{\varepsilon}_4) - f(e_1 \tilde{\varepsilon}_1) f(e_2 \tilde{\varepsilon}_2) f(-e_3 \tilde{\varepsilon}_3) f(-e_4 \tilde{\varepsilon}_4)] , \quad (55)$$

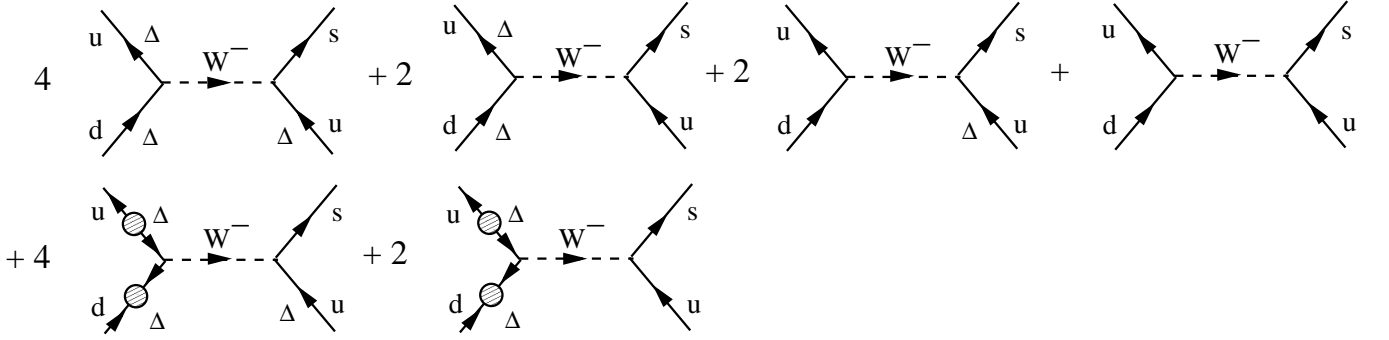


FIG. 2: Contributions to the process $d + u \rightarrow u + s$. The four diagrams in the first row contain 3, 2, 1, and 0 gapped fermions, respectively (a gapped fermion is marked by Δ at the respective lines). The combinations of quarks of the first two diagrams in the first row allow for nonvanishing contributions of anomalous propagators. These are shown in the second row (a condensate insertion is represented by a hatched circle).

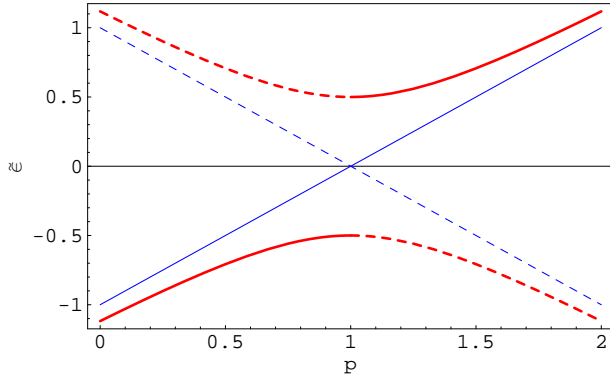


FIG. 3: (Color online) Thick (red) lines: gapped modes. Thin (blue) lines: ungapped modes. Solid lines: $+\tilde{\epsilon}$. Dashed lines: $-\tilde{\epsilon}$. The quantities are given in arbitrary units, $\mu = 1$. This figure illustrates the new variables introduced in Eq. (54), which are advantageous for the discussion of the various subprocesses, as explained below Eq. (57).

and for the contribution of the anomalous propagators

$$\tilde{\Gamma}_d^{r_1 r_2 r_3 r_4} \equiv \frac{G_F^2 V_{ud}^2 V_{us}^2}{16\pi^5} \sum_{e_1 e_2 e_3 e_4} \int_{p_1 p_2 p_3 p_4} \tilde{I}(p_1, p_2, p_3, p_4) \frac{e_1 \Delta}{2\tilde{\epsilon}_1} \tilde{B}_2^{e_2} \tilde{B}_3^{e_3} \frac{e_4 \Delta}{2\tilde{\epsilon}_4} \delta(e_1 \tilde{\epsilon}_1 + e_2 \tilde{\epsilon}_2 - e_3 \tilde{\epsilon}_3 - e_4 \tilde{\epsilon}_4 - \delta\mu) \times [f(-e_1 \tilde{\epsilon}_1) f(-e_2 \tilde{\epsilon}_2) f(e_3 \tilde{\epsilon}_3) f(e_4 \tilde{\epsilon}_4) - f(e_1 \tilde{\epsilon}_1) f(e_2 \tilde{\epsilon}_2) f(-e_3 \tilde{\epsilon}_3) f(-e_4 \tilde{\epsilon}_4)] . \quad (56)$$

Because of $\tilde{B}_i^- = 0$ for $\Delta = 0$, only one of the 16 terms, namely $e_1 = \dots = e_4 = 1$, survives in the unpaired phase limit and we immediately obtain for this case

$$\Gamma_d^{\text{unp}} = \frac{9G_F^2 V_{ud}^2 V_{us}^2}{8\pi^5} \int_{p_1 p_2 p_3 p_4} I(p_1, p_2, p_3, p_4) \delta(p_1 + p_2 - p_3 - p_4) \times \{[1 - f(p_1 - \mu)][1 - f(p_2 - \mu)]f(p_3 - \mu_s)f(p_4 - \mu) - f(p_1 - \mu)f(p_2 - \mu)[1 - f(p_3 - \mu_s)][1 - f(p_4 - \mu)]\} , \quad (57)$$

in accordance with Ref. [40]. Note that in the representation of Eq. (50), all 16 subprocesses contribute even in the unpaired phase (of course yielding the same result (57)). It is easy to understand that the quantities in Eq. (54) are more natural to describe the unpaired phase because $\tilde{\epsilon}_i = p_i - \mu_i$ describes particle excitations for all momenta p_i . In contrast, $\epsilon_i = |p_i - \mu_i|$ describes hole excitations for $p_i < \mu$ and particle excitations for $p_i > \mu_i$. This distinction between particles and holes is not possible in the quasiparticle description of the superconducting phase. However, also in the 2SC phase the new representation is instructive since it reveals the processes that are only possible in a superconductor/superfluid, namely the 15 subprocesses that contain at least one \tilde{B}_i^- . They correspond to processes in which three particles coalesce to one particle (or one particle decays into three) and in which four particles are

annihilated (or created). This is possible because particle number is not conserved. Particles can be created from or deposited into the condensate. Only when there is no condensate, the “conventional” process of two incoming and two outgoing particles is the only possible one. In the next section, we shall study the quantitative contribution of these “exotic” processes to the total rate.

As a result of this subsection, let us rewrite the collision integral (47) using the following more illustrative notation,

$$\Gamma_d = 4\Gamma_d^{e_1 e_2 e_4}(\Delta, \Delta, \Delta) + 2\Gamma_d^{e_1 e_4}(\Delta, 0, \Delta) + 2\Gamma_d^{e_2}(0, \Delta, 0) + \Gamma_d(0, 0, 0) + 4\tilde{\Gamma}_d^{e_1 e_2 e_4}(\Delta, \Delta, \Delta) + 2\tilde{\Gamma}_d^{e_1 e_4}(\Delta, 0, \Delta), \quad (58)$$

where summation over the respective $e_i = \pm$ is implied. We shall also use the shorthand notation $\Gamma_d(\Delta, \Delta, \Delta) \equiv \Gamma_d^{e_1 e_2 e_4}(\Delta, \Delta, \Delta)$ etc. where no confusion is possible. This notation shows explicitly how many gapped modes participate in the respective subprocesses. The definitions of the new quantities is clear from comparison with Eq. (47), the sum over e_1, e_2, e_4 originating from Eqs. (55) and (56). Since the s quark (corresponding to e_3) is ungapped, only terms with $e_3 = +1$ survive, and the superscripts e_1, e_2, e_4 as well as the three arguments of the functions Γ_d correspond to the quark flavors d, u_1 , and u_2 . It is clear from the definition that the number of gapped modes determines how many of the 16 subprocesses are nonvanishing. This number can be directly read off from the notation in Eq. (58), i.e., all e_i ’s that are shown explicitly have to be summed over ± 1 , while the missing e_i are set to $+1$, since the contribution for -1 vanishes.

IV. EVALUATION OF THE RATE

The general evaluation of the collision integral has to be done numerically. As a consistency check, let us derive the analytical result in the unpaired phase for zero temperature. In this case, all Fermi distributions in Eq. (57) become step functions,

$$\begin{aligned} \Gamma_d^{\text{unp},0} &= \frac{9G_F^2 V_{ud}^2 V_{us}^2}{8\pi^5} \int_{p_1 p_2 p_3} I(p_1, p_2, p_3, p_1 + p_2 - p_3) \Theta(p_1 + p_2 - p_3) \\ &\times [\Theta(p_1 - \mu)\Theta(p_2 - \mu)\Theta(\mu_s - p_3)\Theta(\mu - p_1 - p_2 + p_3) - \Theta(\mu - p_1)\Theta(\mu - p_2)\Theta(p_3 - \mu_s)\Theta(p_1 + p_2 - p_3 - \mu)] . \end{aligned} \quad (59)$$

Since we assumed that $\delta\mu = \mu_s - \mu > 0$, the second term in square brackets vanishes. (The first three step functions in this term imply $p_1 + p_2 - p_3 < 2\mu - \mu_s$ which, for $\mu_s > \mu$, contradicts the fourth one, implying $p_1 + p_2 - p_3 > \mu$.) Physically, this means that at zero temperature the process only happens in one direction. This direction is given by the sign of $\delta\mu$. The first term in square brackets can be evaluated upon using the definition of the function I in Eq. (D13a). One finds

$$\begin{aligned} \Gamma_d^{\text{unp},0} &= \frac{6}{5\pi^5} G_F^2 V_{ud}^2 V_{us}^2 \int_{\mu}^{\mu_s} dp_3 \int_{\mu}^{p_3} dp_2 \int_{\mu}^{p_3 - p_2 + \mu} dp_1 (p_1 + p_2 - p_3)^3 [(p_1 + p_2)^2 + 3p_3(p_1 + p_2) + 6p_3^2] \\ &= \frac{16}{5\pi^5} G_F^2 V_{us}^2 V_{ud}^2 \left(\mu^5 \delta\mu^3 + \frac{5}{16} \mu^4 \delta\mu^4 - \frac{3}{16} \mu^3 \delta\mu^5 + \frac{1}{32} \mu^2 \delta\mu^6 + \frac{5}{112} \mu \delta\mu^7 - \frac{15}{896} \delta\mu^8 \right) , \end{aligned} \quad (60)$$

which is in agreement with Ref. [40].

We treat all other cases numerically. For the following results we use $\mu = 500$ MeV and $\delta\mu = 10$ MeV. We assume a transition temperature of $T_c = 30$ MeV. Via the relation $T_c/\Delta_0 = e^\gamma/\pi$, where $\gamma \simeq 0.577$ is the Euler-Mascheroni constant, this corresponds to a zero-temperature gap $\Delta_0 \simeq 52.6$ MeV. We shall employ the following model temperature dependence of the gap,

$$\Delta(T) = \Delta_0 \sqrt{1 - \left(\frac{T}{T_c} \right)^2} . \quad (61)$$

We have to compute the collision integrals $\Gamma_d(\Delta_1, \Delta_2, \Delta_4)$ for all combinations of $\Delta_1, \Delta_2, \Delta_4$ shown in Eq. (58). Let us analyse the various subprocesses before we add them up to the total rate. To this end we pick the first term on the right-hand side of Eq. (58), which actually is a sum of 8 subrates. We show the rates of all 8 subprocesses of $\Gamma_d(\Delta, \Delta, \Delta)$ in Fig. 4. The figure shows that, due to symmetries of the collision integral, some of the resulting curves coincide. One obtains four groups, characterized by zero, one, two, and three factors \tilde{B}_i^- in the collision integral (from top to bottom in the figure). In other words, the three lower curves in the right panel describe processes of coalescence or decay of particles, while the upper curve corresponds to a “normal” interaction process of two incoming and two outgoing particles. The left panel shows that this “normal” process is the only one that does not vanish at the transition temperature. Of course, all other processes can only contribute to the rate in the presence of a

condensate. Although smaller in magnitude, these processes cannot be completely neglected for any temperature range since their contribution increases quickly for temperatures decreasing down from T_c . A quantitative analysis shows that the seven processes where at least one of e_1, e_2, e_4 equals -1 add up to about 30% of the total rate at $T/T_c \simeq 0.9$, and their relative contribution increases monotonically with decreasing temperature.

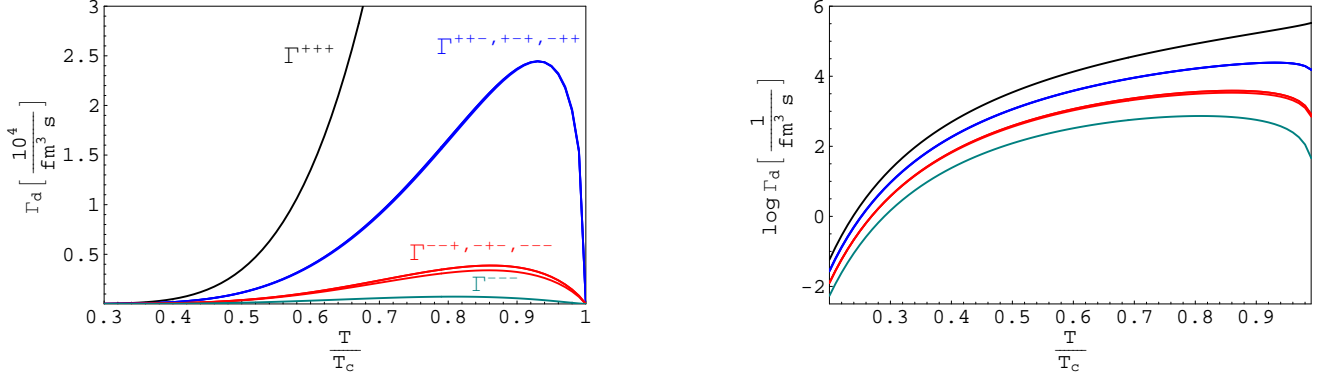


FIG. 4: (Color online) Subprocesses $\Gamma_d^{e_1 e_2 e_4}(\Delta, \Delta, \Delta)$ on a linear scale (left panel) and a logarithmic scale (right panel). The uppermost (black) line corresponds to the process Γ_d^{+++} with two incoming and two outgoing particles. All other processes include creation or annihilation of particles from the condensate. These processes are only possible in the superconducting phase and thus vanish at the critical temperature.

An evaluation of the 8 subprocesses from Eq. (56), $\tilde{\Gamma}_d(\Delta, \Delta, \Delta)$, shows that their contribution is of the order of the processes $\Gamma_d^{--+}(\Delta, \Delta, \Delta)$. Or, to give another quantitative estimate of these processes, we find that $\sum_{e_1 e_2 e_4} \tilde{\Gamma}_d^{e_1 e_2 e_4}(\Delta, \Delta, \Delta) < \Gamma_d^{--+}(\Delta, \Delta, \Delta)$. Therefore, one can neglect these contributions, i.e., we may use $\Gamma_d(\Delta_1, \Delta_2, \Delta_4)$ for the almost identical rate $\Gamma_d(\Delta_1, \Delta_2, \Delta_4) + \tilde{\Gamma}_d(\Delta_1, \Delta_2, \Delta_4)$.

For the rates $\Gamma_d^{e_1, e_4}(\Delta, 0, \Delta)$ and $\Gamma_d^{e_2}(0, \Delta, 0)$ there are 4 and 2 subprocesses, respectively. We do not show the results for these subprocesses explicitly, since the corresponding plots are very similar to the ones in Fig. 4.

After having discussed the subprocesses for a given number of gapped fermions, we shall now compare the rates for processes with different numbers of gapped fermions. I.e., so far we have picked the first of the terms on the right-hand side of Eq. (58) and analyzed the subprocesses hidden in this term. Now we shall compare the different terms in this equation with each other. This is done in Fig. 5. Every curve in this figure corresponds to the rate of a given number of participating gapped fermions, where the number of gapped fermions increases from the top to the bottom curve. One sees that all rates containing at least one gapped fermion are strongly suppressed for small temperatures. This suppression can easily be extracted analytically, see Appendix E. For $\delta\mu < \Delta_0$, the leading behavior for small temperatures is

$$\Gamma_d(\Delta, \Delta, \Delta) \sim e^{-(2\Delta - \delta\mu)/T}, \quad \Gamma_d(\Delta, 0, \Delta) \sim e^{-\Delta/T}, \quad \Gamma_d(0, \Delta, 0) \sim e^{-(\Delta - \delta\mu)/T}. \quad (62)$$

In Appendix E, also the behavior for $\delta\mu > \Delta_0$, is derived (although this regime is not relevant in the present context). From the suppression due to the gap (62) we conclude that for small temperatures, we may approximate the total 2SC rate by the contribution of ungapped fermions, $\Gamma_d \simeq \Gamma_d(0, 0, 0)$ [41]. In Fig. 6 we see that this approximation starts to break down for temperatures $T \gtrsim 10 \text{ MeV} \simeq 0.3 T_c$.

V. RESULTS FOR THE BULK VISCOSITY

In this section, we compute the bulk viscosity of 2SC quark matter as a function of temperature. We first discuss the role of the subprocesses in Sec. V A before we compare the total bulk viscosity of the 2SC phase with that of unpaired quark matter in Sec. V B. We make use of the expression for the bulk viscosity derived in Sec. II, see Eq. (21). This equation shows that we need the quantities ω , B , C , and $\gamma = C\lambda$. For the coefficients B and C , see definitions (10) and (14) and Table I; we use a strange mass $m_s = 100 \text{ MeV}$ and a chemical potential of $\mu = 500 \text{ MeV}$. In order to determine γ , we need the results for the rate Γ_d , presented in the previous section. Remember that, in the derivation of the bulk viscosity, leading to Eq. (21), we have assumed the rate to be linear in $\delta\mu$, see Eq. (8). This linear approximation is, for any given temperature T , valid for a sufficiently small $\delta\mu$. Physically, this means that we

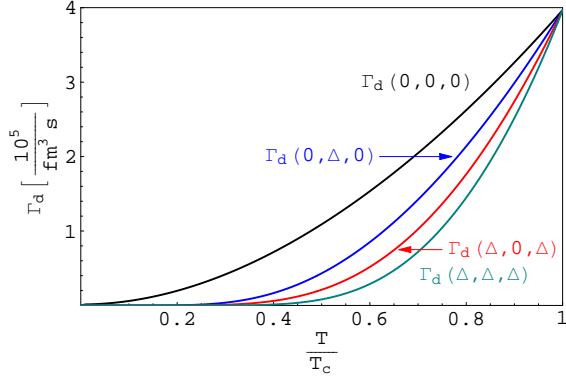


FIG. 5: (Color online) Contributions to the 2SC rate, separated by the number of participating gapped fermions. The more fermions are gapped, the lower is the rate of the corresponding subprocess. The lowest (green) curve is the sum of the subprocesses shown in Fig. 4. The sum of all lines in this figure is the total rate Γ_d in the 2SC phase.

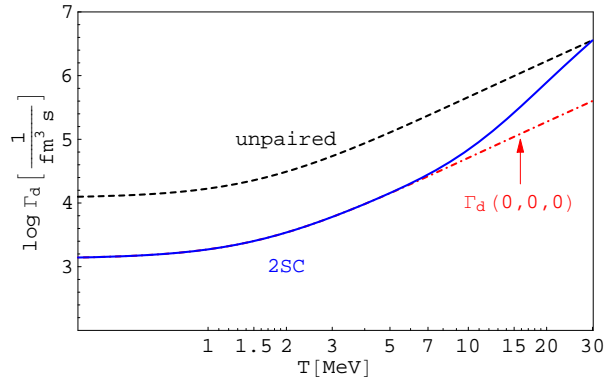


FIG. 6: (Color online) Total 2SC rate (solid, blue) obtained from Eq. (58) compared to the unpaired phase rate $\Gamma_d^{\text{unp}} = 9\Gamma_d(0,0,0)$ (dashed, black) and the rate $\Gamma_d(0,0,0)$ (dashed-dotted, red) on a logarithmic temperature scale (remember $T_c = 30$ MeV). For small temperatures, the result approaches the zero-temperature result (which, in the case of the unpaired phase, is given by Eq. (60)). The 2SC rate is well approximated by $\Gamma_d(0,0,0)$ up to $T \simeq 0.3 T_c$. Above this temperature, effects of the gapped modes are not negligible. For all temperatures, the rate of the 2SC phase is smaller than that of the unpaired phase. In Sec. V we shall see that this is not true for the bulk viscosity.

assume the volume oscillation $\delta V_0/V_0$ to be sufficiently small, because the magnitude of $\delta\mu$ is proportional to $\delta V_0/V_0$, see Eq. (19). Technically, we have to compute the rate Γ_d at a sufficiently small $\delta\mu$ such that we can determine λ , and thus the characteristic frequency γ , via $\lambda = \Gamma_d/\delta\mu$. (Hence, we cannot necessarily use the numerical values from the previous section which have been obtained for a fixed $\delta\mu = 10$ MeV.)

A. Contribution of subprocesses to the bulk viscosity

Before we turn to the final results for the 2SC phase, let us discuss the contribution of the subprocesses. As we have discussed in Sec. IV, the rates of the subprocesses depend on the number of gapped fermions that participate in the process. In Fig. 5 we have shown these rates, namely $\Gamma_d(\Delta, \Delta, \Delta)$, $\Gamma_d(\Delta, 0, \Delta)$, $\Gamma_d(0, \Delta, 0)$, and $\Gamma_d(0, 0, 0)$. In Fig. 7, we show four different bulk viscosities, assuming (fictitiously) that the bulk viscosity solely depends on each of these rates. The different suppression of the rates as a function of temperature leads to different temperatures at which the bulk viscosity becomes maximal (see Sec. V B for a further discussion of the maxima of the viscosity). What do we conclude for the 2SC bulk viscosity from these curves? Or, in other words, how do these curves “add up” to yield the total bulk viscosity as a function of temperature? To answer this question, remember the analogy between periodically expanding and contracting quark matter and an electric circuit with alternating voltage, see Sec. II. In that section we explained that one may think of a “capacitance” that behaves like the inverse of the rate $1/\lambda$, see Eq. (16). If

the rate consists of a sum of several distinct substrates (as is the case in 2SC quark matter), small substrates can be neglected if there is a large, dominating substrate. The resulting “capacitance” is then determined by the dominating substrate, just as in an electric circuit with capacitors C_1, C_2 in series where $1/C_{\text{total}} = 1/C_1 + 1/C_2$. Therefore, the bulk viscosity of 2SC quark matter is dominated by the subprocess of ungapped fermions, $\Gamma_d(0, 0, 0)$, although each of the subprocesses with gapped fermions would, for certain temperatures and in the absence of $\Gamma_d(0, 0, 0)$, yield a much *larger* bulk viscosity (as can be seen by comparing Fig. 7 with the final results, Fig. 8). Note that it is crucial for this argument that all subprocesses (all “capacitors”) affect one single chemical nonequilibrium (one single “current”), characterized by $\delta\mu = \mu_s - \mu_d$.

In Appendix B we show how this argument is altered when there is more than one independent $\delta\mu$. To illustrate this point let us assume for a moment that the strong interactions, which can change the color of the quarks, are no faster than the weak interactions. In this case, we must not consider the “accumulated” process $u + d \leftrightarrow u + s$, but nine processes $iu + jd \leftrightarrow ju + is$, where i and j each stand for one of three colors, $i, j = \text{red, green, blue}$. And, importantly, there is not only a single $\delta\mu$, but nine $\delta\mu_n$ ’s, one for each of these subprocesses. In this picture, the bulk viscosity is sensitive to the re-equilibration of each of the nine out-of-equilibrium quantities $\delta\mu_n$, leading to a significantly different result. Roughly speaking, the result would be a curve that follows all the maxima of the curves in Fig. 7. However, this picture is unphysical since it ignores the effect of the strong interactions. They provide color-changing processes on a time scale much faster than the weak processes. We show in Appendix B that, after taking into account the strong processes, one arrives at the simpler picture that has been used in Sec. II: There is only a single out-of-equilibrium quantity $\delta\mu$ and the substrates add up like capacitors in series in an electric circuit. Then, the physical result for the total bulk viscosity is given by Fig. 8, which we discuss in the following.

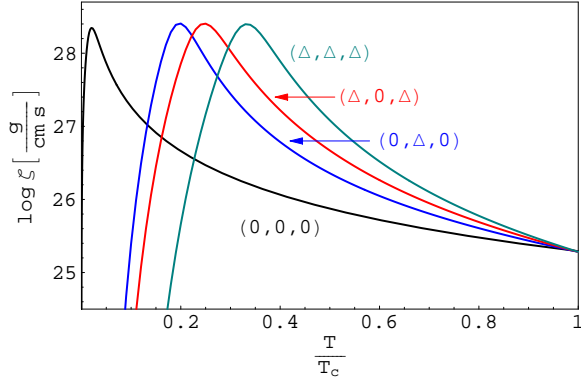


FIG. 7: (Color online) Bulk viscosities calculated as if the only equilibration processes were those that contribute to the $\Gamma_d(0, 0, 0)$ substrate (black), the $\Gamma_d(0, \Delta, 0)$ substrate (blue), the $\Gamma_d(\Delta, 0, \Delta)$ substrate (red), and $\Gamma_d(\Delta, \Delta, \Delta)$ substrate (green). We fixed $\omega/(2\pi) = 10^3 \text{ s}^{-1}$ and $\mu = 500 \text{ MeV}$. The temperature scale is linear.

B. Bulk viscosity of 2SC quark matter

In Fig. 8 we show the bulk viscosity for unpaired and 2SC quark matter for two different oscillation frequencies $\omega/(2\pi) = 200 \text{ s}^{-1}$ (left panel) and $\omega/(2\pi) = 1000 \text{ s}^{-1}$ (right panel). We now explain the features of these plots.

- The bulk viscosity peaks at a particular temperature. This is expected from Eq. (21): the bulk viscosity as a function of the rate γ , for a fixed external frequency ω , has a maximum at $\gamma = \omega$, when the frequency of the externally imposed compression matches the microscopic equilibration rate. Since the microscopic rate $\gamma(T)$ is a monotonic function of the temperature (see results of the previous section), we see this maximum when we compute the bulk viscosity as a function of T .
- The peak viscosities are easily determined by setting $\gamma = \omega$ in Eq. (21),

$$\zeta_{\text{max}} = \frac{B^2}{2C\omega}, \quad (63)$$

i.e., they are independent of the microscopic equilibration rate. In particular, this simple relation explains the larger maximum values of the viscosity in the left panel of Fig. 8 compared to the right panel because of the different values of ω . In general, ζ_{max} is different for unpaired and 2SC quark matter because the values of B and

C differ from phase to phase, see Table I. For the chosen values of m_s and Δ , the peak values happen to be almost identical.

- The 2SC phase has its maximum viscosity at a higher temperature than the unpaired phase; near and above this temperature (up to $T \simeq 2T_c/3$), the 2SC phase has a larger viscosity than the unpaired phase. This follows from the fact that $\gamma(T)$ is monotonically increasing, but the 2SC phase has a slower equilibration rate. At very low temperatures both rates are slow, and the higher rate is closer to ω , so the unpaired phase has higher viscosity [41]. At higher temperatures, both rates are above ω , but now the slower rate is closer to ω , so the 2SC phase has higher viscosity.
- At low temperature, up to temperatures where the viscosity of the unpaired phase peaks, the unpaired and 2SC viscosities differ by a constant factor (the two lines are parallel on our logarithmic plot). This follows from $\zeta \propto \gamma$ for $\gamma \ll \omega$ and the results of the previous section where we have shown that for sufficiently small temperatures, roughly $T \lesssim 0.3 T_c$ (see Fig. 6), the rates simply differ by a factor 9 because the contribution of the gapped modes can be neglected. Also for temperatures larger than the temperature at which the viscosity of the 2SC phase peaks up to $T \simeq 10$ MeV, the viscosities differ by a constant factor. However, they are now in reversed order since $\zeta \propto 1/\gamma$ for $\gamma \gg \omega$.
- At the critical temperature, here chosen to be $T_c = 30$ MeV, the rates of the two phases become the same (the 2SC gap vanishes). However, due to the “locking” of Fermi surfaces in the 2SC phase and the resulting difference in the coefficients entering the viscosity, the viscosities are different. From the values in Table I we conclude $\zeta_{\text{unp}}(T_c)/\zeta_{\text{2SC}}(T_c) = 9/4 + \mathcal{O}(m_s^2/\mu^2)$, in agreement with the results shown in Fig. 8.

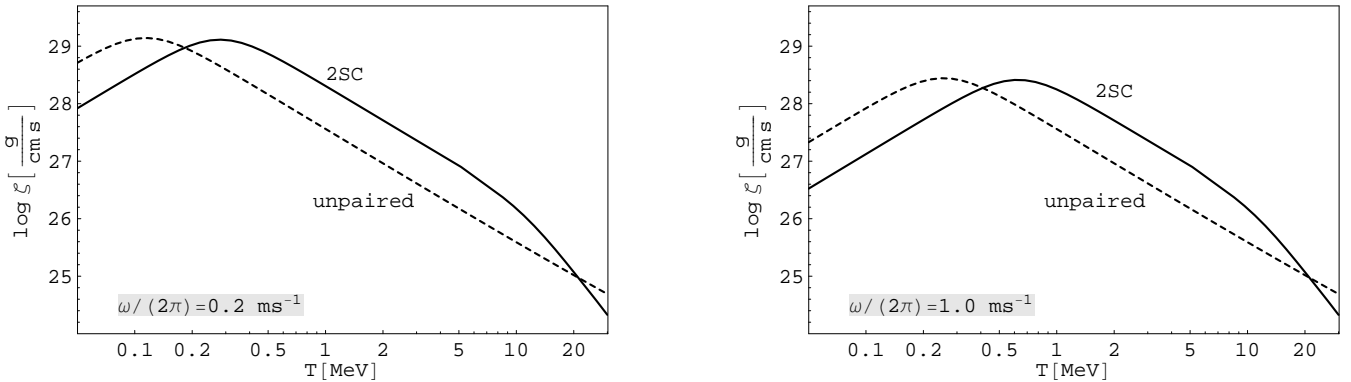


FIG. 8: Bulk viscosities as a function of temperature for 2SC phase (solid line) and unpaired phase (dashed line), for a chemical potential $\mu = 500$ MeV, and oscillation frequencies $\omega/(2\pi) = 0.2 \text{ ms}^{-1}$ (left panel) and $\omega/(2\pi) = 1.0 \text{ ms}^{-1}$ (right panel). Note that temperature is plotted on a logarithmic scale. For $0.2 \text{ MeV} \lesssim T \lesssim 20 \text{ MeV}$ and $0.4 \text{ MeV} \lesssim T \lesssim 20 \text{ MeV}$, respectively, 2SC has a higher bulk viscosity.

VI. CONCLUSIONS

We have computed the bulk viscosity of three-flavor color-superconducting quark matter in the 2SC phase originating from the nonleptonic weak process $u + d \leftrightarrow u + s$. To this end, we have presented a detailed calculation of the rate for this process for arbitrary temperatures. Since 2SC quark matter contains ungapped strange quarks as well as gapped and ungapped up and down quarks, this process contains several subprocesses. Each of these subprocesses that contains at least one gapped quasiparticle mode can be further divided into “subsubprocesses” which are similar to the ones in ordinary superfluids such as ${}^3\text{He}$. In both color superconductors and ${}^3\text{He}$, these subsubprocesses allow for creation and annihilation of quasiparticles from the condensate. Therefore, the process $u + d \leftrightarrow u + s$ has contributions from decay and coalescence processes. We have presented a formal derivation of the total rate, starting from a kinetic equation and making use of the microscopic fermion propagators, resulting in an expression that naturally contains all these contributions. Our results are not only interesting for the special case of the 2SC phase but also, because of the multitude of subprocesses, provide a general quantitative analysis for the effect of a fermion condensate on the considered nonleptonic process.

We have evaluated the rate numerically, observing the expected exponential suppressions for small temperatures. For subprocesses with three gapped modes we find a suppression of the form $e^{-2\Delta/T}$, while two or one gapped mode(s)

yield $e^{-\Delta/T}$. Upon evaluating the collision integral for temperatures up to the superconducting transition temperature, we have also studied the temperature regime where the exponential functions are no longer valid approximations for the rate.

The results for the rate, which translate into a typical time scale of the weak process, have been used to compute the bulk viscosity as a function of temperature for a given external oscillation frequency, chosen to be of order 1 kHz, which corresponds to the fastest rotation rate observed for pulsars. We have pointed out that the bulk viscosity is the response of the quark system to this external oscillation just as an electric circuit responds to an external alternating voltage by an induced current. In this sense, we have identified a “resistance” and a “capacitance” of the quark system in terms of the microscopic process. Using this analogy, it is easy to understand that the behavior of the bulk viscosity assumes a maximum when the microscopic time scale matches that of the external frequency.

Our calculations show that, for a transition temperature of $T_c = 30$ MeV and oscillation frequencies in the kHz range, the bulk viscosity of 2SC quark matter is larger than that of unpaired quark matter over a wide temperature range. This range is approximately given by $T_c/30 < T < 2T_c/3$ for an oscillation period of one millisecond. For longer oscillation periods, this range is even larger. As discussed above, this is because in that temperature range the slower equilibration rate of 2SC matter resonates better with kHz frequency oscillations than does the faster equilibration rate of unpaired quark matter. This result has potential physical implications for the behavior of the star early in its life, before its internal temperature drops below about 1 MeV. It is also interesting to note that at these early times neutrinos are trapped, and the resultant lepton number chemical potential can favor a 2SC phase with strange quarks [19] (but see also [42]). Moreover, bulk viscosity is likely to be the dominant factor for damping of potentially unstable r -modes in this very temperature regime [23, 27]. Although the star cools down below 1 MeV within days, this short time might potentially be long enough for instabilities to grow and spin down the star drastically [43]. For hot newly born stars, we have thus found that quark Cooper pairing actually works in favor of damping of unstable modes. For much smaller temperatures, $T \lesssim 0.1$ keV, shear viscosity effects become important, and Cooper pairing is expected to reduce the shear viscosity and thus the damping of the unstable modes [41]. We have found a similar effect for the bulk viscosity: for sufficiently small temperatures, $T < T_c/30$, the bulk viscosity of 2SC quark matter is smaller than that of unpaired quark matter. Besides the damping of unstable rotational modes, bulk viscosity is also an important quantity for time scales of radial pulsation of compact stars [44]. Our results can serve as an ingredient for calculations addressing the viscous damping of these pulsations.

Finally, we emphasize that the results for the bulk viscosity in the 2SC phase cannot be extrapolated to the CFL phase. In this phase, all fermions acquire a gap in their energy spectrum and thus the rate of the process $u + d \leftrightarrow u + s$ will be smaller than in the 2SC phase. In particular, this rate will be exponentially suppressed for small temperatures. However, kaons (which have nonzero strangeness) serve as a more effective source for re-equilibration, and their contribution to the bulk viscosity has to be taken into account [45].

Acknowledgments

The authors like to thank M. Braby, P. Jaikumar, S. Reddy, D. Rischke, B. Sa’d, and I. Shovkovy for valuable discussions and acknowledge support by the U.S. Department of Energy under contracts DE-FG02-91ER50628 and DE-FG01-04ER0225 (OJI).

APPENDIX A: BULK VISCOSITY INCLUDING LEPTONIC PROCESSES

In this appendix, we derive an expression for the bulk viscosity which is valid for a system that not only converts s into u quarks via the non-leptonic process considered in the main part of the paper, but also contains leptonic processes. We shall consider the following three processes, employing the linear approximation for the several rates as in Sec. II,

$$u + d \leftrightarrow u + s, \quad \Gamma_1 = \lambda_1 \delta\mu_1, \quad (\text{A1a})$$

$$u + e \leftrightarrow d + \nu, \quad \Gamma_2 = \lambda_2 \delta\mu_2, \quad (\text{A1b})$$

$$u + e \leftrightarrow s + \nu, \quad \Gamma_3 = \lambda_3 \delta\mu_3. \quad (\text{A1c})$$

The quantities Γ_1 , λ_1 , and $\delta\mu_1$ correspond to Γ_d , λ , and $\delta\mu$ in Sec. II. In chemical equilibrium, $\delta\mu_1 = \delta\mu_2 = \delta\mu_3 = 0$. Out of equilibrium, the quantities

$$\delta\mu_1 = \mu_s - \mu_d, \quad (\text{A2a})$$

$$\delta\mu_2 = \mu_d - \mu_u - \mu_e, \quad (\text{A2b})$$

$$\delta\mu_3 = \mu_s - \mu_u - \mu_e = \delta\mu_1 + \delta\mu_2, \quad (\text{A2c})$$

are nonzero (we assume $\mu_\nu = 0$). Note that there are only two independent $\delta\mu$'s. According to the above microscopic processes, the densities for electrons and quarks change as follows,

$$\frac{dn_e}{dt} = \Gamma_2 + \Gamma_3 = \lambda_3 \delta\mu_1 + (\lambda_2 + \lambda_3) \delta\mu_2, \quad (\text{A3a})$$

$$\frac{dn_d}{dt} = \Gamma_1 - \Gamma_2 = \lambda_1 \delta\mu_1 - \lambda_2 \delta\mu_2, \quad (\text{A3b})$$

$$\frac{dn_s}{dt} = -\Gamma_1 - \Gamma_3 = -\frac{dn_d}{dt} - \frac{dn_e}{dt}, \quad (\text{A3c})$$

$$\frac{dn_u}{dt} = \Gamma_2 + \Gamma_3 = \frac{dn_e}{dt}. \quad (\text{A3d})$$

We can thus express all density changes in terms of the changes in n_e and n_d . Analogous to Sec. II, we write the pressure as

$$\begin{aligned} p(t) &= p_0 + \left(\frac{\partial p}{\partial V} \right)_0 \delta V + \left(\frac{\partial p}{\partial n_e} \right)_0 \delta n_e + \left(\frac{\partial p}{\partial n_d} \right)_0 \delta n_d + \left(\frac{\partial p}{\partial n_s} \right)_0 \delta n_s + \left(\frac{\partial p}{\partial n_u} \right)_0 \delta n_u \\ &= p_0 + \left(\frac{\partial p}{\partial V} \right)_0 \delta V + (B_1 + B_2) \delta n_e + B_1 \delta n_d, \end{aligned} \quad (\text{A4})$$

where

$$B_1 \equiv \left(n_d \frac{\partial \mu_d}{\partial n_d} \right)_0 - \left(n_s \frac{\partial \mu_s}{\partial n_s} \right)_0, \quad (\text{A5a})$$

$$B_2 \equiv \left(n_u \frac{\partial \mu_u}{\partial n_u} \right)_0 + \left(n_e \frac{\partial \mu_e}{\partial n_e} \right)_0 - \left(n_d \frac{\partial \mu_d}{\partial n_d} \right)_0, \quad (\text{A5b})$$

and we have made use of the relations between the various densities given in Eqs. (A3). For the purpose of this appendix, it is sufficient to consider unpaired quark matter. In the 2SC phase, B_1 and B_2 would have additional terms due to the pairing of u and d quarks. Since the conclusions of this appendix do not depend on the values of B_1 and B_2 we may for simplicity proceed without taking into account the effects of pairing. Then, the average power dissipation, cf. Eq. (9), is

$$\left\langle \frac{dW}{dt} \right\rangle = a_1 \langle \delta\mu_1(t) \delta v(t) \rangle + a_2 \langle \delta\mu_2(t) \delta v(t) \rangle, \quad (\text{A6})$$

where we abbreviated

$$a_1 \equiv B_1 \lambda_1 + (B_1 + B_2) \lambda_3, \quad (\text{A7a})$$

$$a_2 \equiv B_2 \lambda_2 + (B_1 + B_2) \lambda_3. \quad (\text{A7b})$$

The changes in the chemical potentials are derived as in Sec. II, cf. Eqs. (11) and (12),

$$\frac{\partial \delta\mu_i}{\partial t} = B_i \frac{\partial \delta v}{\partial t} - \alpha_i \delta\mu_1 - \beta_i \delta\mu_2, \quad i = 1, 2, \quad (\text{A8})$$

where

$$\alpha_i \equiv C_i^d \lambda_1 + C_i^e \lambda_3, \quad (\text{A9a})$$

$$\beta_i \equiv C_i^e (\lambda_2 + \lambda_3) - C_i^d \lambda_2, \quad (\text{A9b})$$

with

$$C_1^d \equiv \left(\frac{\partial \mu_d}{\partial n_d} \right)_0 + \left(\frac{\partial \mu_s}{\partial n_s} \right)_0, \quad C_1^e \equiv \left(\frac{\partial \mu_s}{\partial n_s} \right)_0, \quad (\text{A10a})$$

$$C_2^d \equiv -\left(\frac{\partial \mu_d}{\partial n_d} \right)_0, \quad C_2^e \equiv \left(\frac{\partial \mu_u}{\partial n_u} \right)_0 + \left(\frac{\partial \mu_e}{\partial n_e} \right)_0. \quad (\text{A10b})$$

The single differential equation (12) thus has become a system of two coupled differential equations (A8). With the ansatz $\delta\mu_i = \text{Re}(\delta\mu_i^0 e^{i\omega t})$ we may reduce the system of differential equations to an algebraic set of four linear equations for the four variables $\text{Re} \delta\mu_1^0, \text{Im} \delta\mu_1^0, \text{Re} \delta\mu_2^0, \text{Im} \delta\mu_2^0$,

$$\omega \text{Re} \delta\mu_i^0 = \omega B_i \delta v_0 - \alpha_i \text{Im} \delta\mu_1^0 - \beta_i \text{Im} \delta\mu_2^0, \quad (\text{A11a})$$

$$\omega \text{Im} \delta\mu_i^0 = \alpha_i \text{Re} \delta\mu_1^0 + \beta_i \text{Re} \delta\mu_2^0. \quad (\text{A11b})$$

From Eq. (A6) and $\delta v(t) = \delta v_0 \cos \omega t$ we conclude that only the real parts of the complex amplitudes $\delta\mu_i^0$ enter the power dissipation. They are given by

$$\text{Re} \delta\mu_1^0 = \delta v_0 \omega^2 \frac{B_1(\beta_2^2 + \alpha_2 \beta_1) - B_2 \beta_1(\alpha_1 + \beta_2) + B_1 \omega^2}{(\alpha_2 \beta_1 - \alpha_1 \beta_2)^2 + (2\alpha_2 \beta_1 + \alpha_1^2 + \beta_2^2) \omega^2 + \omega^4}, \quad (\text{A12a})$$

$$\text{Re} \delta\mu_2^0 = \delta v_0 \omega^2 \frac{B_2(\alpha_1^2 + \alpha_2 \beta_1) - B_1 \alpha_2(\alpha_1 + \beta_2) + B_2 \omega^2}{(\alpha_2 \beta_1 - \alpha_1 \beta_2)^2 + (2\alpha_2 \beta_1 + \alpha_1^2 + \beta_2^2) \omega^2 + \omega^4}. \quad (\text{A12b})$$

Consequently, Eq. (A6) and the definition (1) yield the bulk viscosity

$$\zeta = a_1 \frac{\text{Re} \delta\mu_1^0}{\delta v_0 \omega^2} + a_2 \frac{\text{Re} \delta\mu_2^0}{\delta v_0 \omega^2} = \frac{P_1 + P_2 \omega^2}{Q_1 + Q_2 \omega^2 + \omega^4}, \quad (\text{A13})$$

where

$$\begin{aligned} P_1 \equiv & (\lambda_1 \lambda_2 + \lambda_1 \lambda_3 + \lambda_2 \lambda_3) \left(B_1^2 \{ (C_2^d - C_2^e)[C_2^d \lambda_2 - C_2^e(\lambda_2 + \lambda_3)] + (C_1^e - C_1^d)(C_2^d \lambda_1 + C_2^e \lambda_3) \} \right. \\ & + B_1 B_2 \{ (C_1^d - C_1^e - C_2^d)[C_1^d \lambda_1 + (C_2^e - C_2^d)\lambda_2] + [C_1^e(C_1^d - C_1^e + C_2^d) - C_2^e(C_1^d + C_1^e + C_2^d)]\lambda_3 \} \\ & \left. + B_2^2[(C_1^d)^2 \lambda_1 + (C_1^e - C_1^d)C_2^d \lambda_2 + (C_1^d + C_2^d)C_1^e \lambda_3] \right), \end{aligned} \quad (\text{A14a})$$

$$P_2 \equiv B_1^2 \lambda_1 + B_2^2 \lambda_2 + (B_1 + B_2)^2 \lambda_3, \quad (\text{A14b})$$

$$Q_1 \equiv (\lambda_1 \lambda_2 + \lambda_1 \lambda_3 + \lambda_2 \lambda_3)(C_1^e C_2^d - C_1^d C_2^e)^2, \quad (\text{A14c})$$

$$Q_2 \equiv (C_1^d \lambda_1 + C_1^e \lambda_3)^2 + 2(C_2^d \lambda_1 + C_2^e \lambda_3)[C_1^e(\lambda_2 + \lambda_3) - C_1^d \lambda_2] + [C_2^d \lambda_2 - C_2^e(\lambda_2 + \lambda_3)]^2. \quad (\text{A14d})$$

With the densities (of unpaired quark matter) $n_{u/d} = \mu_{u/d}^3 / \pi^2$, $n_s = (\mu_s^2 - m_s^2)^{3/2} / \pi^2$, and $n_e = \mu_e^3 / (3\pi^2)$ we have

$$B_1 = \frac{m_s^2}{3\mu_s}, \quad B_2 = 0, \quad (\text{A15a})$$

$$C_1^d = \frac{\pi^2}{3\mu_s^2} \left(1 + \frac{\mu_s}{\sqrt{\mu_s^2 - m_s^2}} \right), \quad C_1^e = \frac{\pi^2}{3\mu_s \sqrt{\mu_s^2 - m_s^2}}, \quad (\text{A15b})$$

$$C_2^d = -\frac{\pi^2}{3\mu_s^2}, \quad C_2^e = \frac{\pi^2}{3} \left(\frac{1}{\mu_u^2} + \frac{3}{\mu_e^2} \right). \quad (\text{A15c})$$

From the definitions it is clear that B_1 and C_1^d correspond to B and C in Sec. II, respectively. The result (A13) together with the definitions (A14) shows that the three processes are entangled in a complicated way. Let us consider some limit cases in which the processes disentangle. In particular, we are interested in the case $\lambda_1 \gg \lambda_2, \lambda_3$, since we expect the rates for the leptonic processes to be much smaller than the rate for the non-leptonic process. In this case,

$$\zeta \simeq B_1^2 \lambda_1 \frac{\lambda_1(\lambda_2 + \lambda_3)(C_1^d - C_1^e)C_1^d + \omega^2}{\lambda_1^2(\lambda_2 + \lambda_3)^2(C_1^e C_2^d - C_1^d C_2^e)^2 + (C_1^d \lambda_1)^2 \omega^2 + \omega^4}. \quad (\text{A16})$$

In order to obtain some qualitative insight we have to compare the inverse time scale ω with the inverse time scales set by λ_1 , λ_2 , and λ_3 . For simplicity, let us set $\lambda_2 = \lambda_3$. As a rough estimate, we shall assume that the factors containing one or several C 's all contribute by a factor $1/\mu_s^2$, i.e., $C_1^d - C_1^e \sim C_1^d \rightarrow 1/\mu_s^2$, $C_1^e C_2^d - C_1^d C_2^e \sim (C_1^d)^2 \rightarrow 1/\mu_s^4$. Then, the relevant inverse time scales

$$\gamma_1 \equiv \frac{\lambda_1}{\mu_s^2}, \quad \gamma_2 \equiv \frac{\lambda_2}{\mu_s^2} \quad (\text{A17})$$

are, for fixed μ_s , indeed set solely by the corresponding rates of the non-leptonic and leptonic processes, respectively, and we can write

$$\zeta \sim \gamma_1 \frac{\gamma_1 \gamma_2 + \omega^2}{\gamma_1^2 \gamma_2^2 + \gamma_1^2 \omega^2 + \omega^4}. \quad (\text{A18})$$

order of time scales	ζ
$\omega \gg \gamma_1 \gg \gamma_2$	γ_1/ω^2
$\omega \simeq \gamma_1 \gg \gamma_2$	$\gamma_1/(\gamma_1^2 + \omega^2)$
$\gamma_1 \gg \omega \gg \gamma_2$	$\gamma_2/\omega^2 + 1/\gamma_1$
$\gamma_1 \gg \omega \simeq \gamma_2$	$\gamma_2/(\gamma_2^2 + \omega^2)$
$\gamma_1 \gg \gamma_2 \gg \omega$	$1/\gamma_2$

TABLE III: Qualitative behavior of the bulk viscosity ζ for different limit cases in which the time scales given by the external oscillation frequency ω , the non-leptonic process γ_1 , and the leptonic process γ_2 are clearly separated.

Obviously, it is incorrect to neglect the much slower process in general. Which process can be neglected rather depends on ω . In particular, we may consider several limit cases in which the time scales clearly separate, see Table III. The general and plausible conclusion from this table is that the bulk viscosity is dominated by the process whose time scale is closest to the time scale set by the external oscillation. (Note that this is in contrast to subprocesses which contribute to one single $\delta\mu$, as considered in the main part of the paper. In this case, the fastest subprocess dominates the bulk viscosity even if there is a slower subprocess which, in the absence of the fast one, would produce a much larger bulk viscosity.) More specifically, the leptonic processes can be neglected in the high frequency limit (first row of Table III) or when the frequency is close to the rate of the non-leptonic process (second row). When the frequency is smaller than the rate of the nonleptonic process, the leptonic processes can only be neglected if its rate is much smaller than the frequency *and* $\omega/\gamma_1 \gg \gamma_2/\omega$, i.e., if the frequency is much closer to the rate of the non-leptonic process than to the rate of the leptonic processes.

APPENDIX B: BULK VISCOSITY INCLUDING STRONG PROCESSES

In this appendix, we show that the expression for the bulk viscosity derived in Sec. II is only correct in the presence of strong processes which are infinitely fast compared to the weak process $u + d \leftrightarrow u + s$. The treatment in Sec. II apparently simplifies the situation because the process $u + d \leftrightarrow u + s$ in fact includes several combinations of quark colors. In principle, one has to treat all possible processes in a way analogous to the method presented in Appendix A, i.e., we have to consider the processes

$$bu + bd \leftrightarrow bu + bs, \quad \Gamma_1 = \lambda_1 \delta\mu_1, \quad (B1a)$$

$$gu + bd \leftrightarrow bu + gs, \quad \Gamma_2 = \lambda_2 \delta\mu_2, \quad (B1b)$$

$$ru + bd \leftrightarrow bu + rs, \quad \Gamma_3 = \lambda_3 \delta\mu_3, \quad (B1c)$$

$$bu + gd \leftrightarrow gu + bs, \quad \Gamma_4 = \lambda_4 \delta\mu_4, \quad (B1d)$$

$$bu + rd \leftrightarrow ru + bs, \quad \Gamma_5 = \lambda_5 \delta\mu_5, \quad (B1e)$$

$$gu + gd \leftrightarrow gu + gs, \quad \Gamma_6 = \lambda_6 \delta\mu_6, \quad (B1f)$$

$$ru + gd \leftrightarrow gu + rs, \quad \Gamma_7 = \lambda_7 \delta\mu_7, \quad (B1g)$$

$$gu + rd \leftrightarrow ru + gs, \quad \Gamma_8 = \lambda_8 \delta\mu_8, \quad (B1h)$$

$$ru + rd \leftrightarrow ru + rs, \quad \Gamma_9 = \lambda_9 \delta\mu_9. \quad (B1i)$$

As in Eqs. (A1) we assign a rate Γ_i to each of the processes and assume these rates to be proportional to the corresponding $\delta\mu_i$. There are nine different processes, because we can assign one of three colors (r, g, b) to each of the two (color-conserving) vertices of the process $u + d \leftrightarrow u + s$. From the results in Secs. III and IV we know that not all of the subprocesses have different rates. Due to the remaining $SU(2)$ color symmetry, we rather have four different rates depending on the number of gapped quasiparticles participating in the process. Using the notation introduced in Eq. (58), we have

$$\Gamma_1 = \Gamma_d(0, 0, 0), \quad (B2a)$$

$$\Gamma_2 = \Gamma_3 = \Gamma_d(0, \Delta, 0), \quad (B2b)$$

$$\Gamma_4 = \Gamma_5 = \Gamma_d(\Delta, 0, \Delta), \quad (B2c)$$

$$\Gamma_6 = \Gamma_7 = \Gamma_8 = \Gamma_9 = \Gamma_d(\Delta, \Delta, \Delta). \quad (B2d)$$

However, for the purpose of this appendix we do not have to make any assumptions for the rates and may treat all nine rates, given by $\lambda_1, \dots, \lambda_9$, as independent.

The various $\delta\mu_i$'s can be written in terms of nine chemical potentials (one for each combination of color and flavor). It turns out that only five of them are independent,

$$\delta\mu_1 = \mu_{bs} - \mu_{bd}, \quad (B3a)$$

$$\delta\mu_2 = \mu_{bu} + \mu_{gs} - \mu_{gu} - \mu_{bd}, \quad (B3b)$$

$$\delta\mu_3 = \mu_{bu} + \mu_{rs} - \mu_{ru} - \mu_{bd} = \delta\mu_2 - \delta\mu_6 + \delta\mu_7, \quad (B3c)$$

$$\delta\mu_4 = \mu_{gu} + \mu_{bs} - \mu_{bu} - \mu_{gd} = \delta\mu_1 - \delta\mu_2 + \delta\mu_6, \quad (B3d)$$

$$\delta\mu_5 = \mu_{ru} + \mu_{bs} - \mu_{bu} - \mu_{rd} = \delta\mu_1 - \delta\mu_2 + \delta\mu_6 - \delta\mu_7 + \delta\mu_9, \quad (B3e)$$

$$\delta\mu_6 = \mu_{gs} - \mu_{gd}, \quad (B3f)$$

$$\delta\mu_7 = \mu_{gu} + \mu_{rs} - \mu_{ru} - \mu_{gd}, \quad (B3g)$$

$$\delta\mu_8 = \mu_{ru} + \mu_{gs} - \mu_{gu} - \mu_{rd} = \delta\mu_6 - \delta\mu_7 + \delta\mu_9, \quad (B3h)$$

$$\delta\mu_9 = \mu_{rs} - \mu_{rd}. \quad (B3i)$$

We may thus choose $\delta\mu_1, \delta\mu_2, \delta\mu_6, \delta\mu_7, \delta\mu_9$, as independent variables. The density changes due to the above processes can be read off from Eqs. (B1),

$$\frac{dn_{ru}}{dt} = \Gamma_3 - \Gamma_5 + \Gamma_7 - \Gamma_8, \quad \frac{dn_{rd}}{dt} = \Gamma_5 + \Gamma_8 + \Gamma_9, \quad \frac{dn_{rs}}{dt} = -\Gamma_3 - \Gamma_7 - \Gamma_9, \quad (B4a)$$

$$\frac{dn_{gu}}{dt} = \Gamma_2 - \Gamma_4 - \Gamma_7 + \Gamma_8, \quad \frac{dn_{gd}}{dt} = \Gamma_4 + \Gamma_6 + \Gamma_7, \quad \frac{dn_{gs}}{dt} = -\Gamma_2 - \Gamma_6 - \Gamma_8, \quad (B4b)$$

$$\frac{dn_{bu}}{dt} = -\Gamma_2 - \Gamma_3 + \Gamma_4 + \Gamma_5, \quad \frac{dn_{bd}}{dt} = \Gamma_1 + \Gamma_2 + \Gamma_3, \quad \frac{dn_{bs}}{dt} = -\Gamma_1 - \Gamma_4 - \Gamma_5. \quad (B4c)$$

Obviously, the total change of the u flavor density vanishes, while the total change of d and s flavor densities has the same absolute value but opposite signs,

$$\frac{dn_u}{dt} = 0, \quad \frac{dn_d}{dt} = -\frac{dn_s}{dt} = \sum_{i=1}^9 \Gamma_i, \quad (B5)$$

where

$$n_i \equiv n_{ri} + n_{gi} + n_{bi}, \quad i = u, d, s. \quad (B6)$$

If the bulk viscosity was determined solely by the above nine subprocesses of the weak process $u+d \leftrightarrow u+s$, we would have to set up a set of five coupled differential equations for the variables $\delta\mu_1, \delta\mu_2, \delta\mu_6, \delta\mu_7, \delta\mu_9$, analogous to Eq. (A8). Its solution would yield the bulk viscosity through an equation analogous to Eq. (A6). We have checked that this procedure would yield a result that differs from the one presented in Sec. V. In particular: While the bulk viscosity given by Eq. (21) is dominated by the fastest of the subprocesses (here $\lambda_1, \dots, \lambda_9$), the setup presented above would potentially allow all subprocesses to contribute significantly to the bulk viscosity (the dominant subprocesses would be determined by the external oscillation frequency ω). In other words, this setup requires all chemical nonequilibria to re-equilibrate separately, and the one that resonates best with the external oscillation gives the largest contribution. In the remainder of this appendix, however, we show that this picture is invalidated by the presence of the strong interactions which allows the fermions to change their color on a much faster time scale than the one given by the weak interaction.

The relevant strong processes change the colors of two different quark flavors. Since there are three pairs of distinct flavors and three pairs of distinct colors, we have to consider the nine processes

$$ru + gd \leftrightarrow gu + rd, \quad ru + gs \leftrightarrow gu + rs, \quad rd + gs \leftrightarrow gd + rs, \quad (B7a)$$

$$ru + bd \leftrightarrow bu + rd, \quad ru + bs \leftrightarrow bu + rs, \quad rd + bs \leftrightarrow bd + rs, \quad (B7b)$$

$$gu + bd \leftrightarrow bu + gd, \quad gu + bs \leftrightarrow bu + gs, \quad gd + bs \leftrightarrow bd + gs. \quad (B7c)$$

Assuming these processes to be infinitely fast (this is equivalent to the assumption that the system be in chemical equilibrium with respect to all of these processes at any time) translates into the following conditions for the chemical potentials,

$$\mu_{ru} + \mu_{gd} - \mu_{gu} - \mu_{rd} = 0, \quad \mu_{ru} + \mu_{gs} - \mu_{gu} - \mu_{rs} = 0, \quad \mu_{rd} + \mu_{gs} - \mu_{gd} - \mu_{rs} = 0, \quad (B8a)$$

$$\mu_{ru} + \mu_{bd} - \mu_{bu} - \mu_{rd} = 0, \quad \mu_{ru} + \mu_{bs} - \mu_{bu} - \mu_{rs} = 0, \quad \mu_{rd} + \mu_{bs} - \mu_{bd} - \mu_{rs} = 0, \quad (B8b)$$

$$\mu_{gu} + \mu_{bd} - \mu_{bu} - \mu_{gd} = 0, \quad \mu_{gu} + \mu_{bs} - \mu_{bu} - \mu_{gs} = 0, \quad \mu_{gd} + \mu_{bs} - \mu_{bd} - \mu_{gs} = 0. \quad (B8c)$$

These equations result in four independent constraints. Consequently, we may express four chemical potentials in terms of the other five, e.g.,

$$\mu_{gd} = \mu_{rd} + \mu_{gu} - \mu_{ru}, \quad \mu_{gs} = \mu_{rs} + \mu_{gu} - \mu_{ru}, \quad (B9a)$$

$$\mu_{bd} = \mu_{rd} + \mu_{bu} - \mu_{ru}, \quad \mu_{bs} = \mu_{rs} + \mu_{bu} - \mu_{ru}. \quad (B9b)$$

Inserting these equations into Eqs. (B3) reduces the number of independent $\delta\mu$'s to one,

$$\delta\mu_1 = \dots = \delta\mu_9 = \mu_{rs} - \mu_{rd} \equiv \delta\mu. \quad (B10)$$

In order to set up the differential equation for this $\delta\mu$, we have to know the dependence of the densities on the remaining chemical potentials (after eliminating μ_{gd} , μ_{bd} , μ_{gs} , μ_{bs} via Eqs. (B9)). Then, in the 2SC phase, the densities of the paired quarks n_{ru} , n_{rd} , n_{gu} , n_{gd} depend on the average chemical potential $(\mu_{rd} + \mu_{gu})/2$. The densities of the unpaired quarks are straightforwardly obtained with Eqs. (B9). Let us, for simplicity, assume that $\mu_{ru} = \mu_{gu} = \mu_{bu} \equiv \mu_u$. Then, we use the flavor densities from Eq. (B6) to obtain

$$\frac{\partial\delta\mu}{\partial t} = - \sum_{i=u,d,s} \left(n_i \frac{\partial\delta\mu}{\partial n_i} \right)_0 \frac{\partial\delta v}{\partial t} + \sum_{i=u,d} \left(\frac{\partial\delta\mu}{\partial n_i} \right)_0 \frac{dn_i}{dt}, \quad (B11)$$

with dn_i/dt given in Eq. (B5). The same procedure is applied to the expression for the power dissipation, cf. Eq. (9). Upon using $\lambda_1 + \dots + \lambda_9 = \lambda$ with λ defined in Eq. (8), we see that the final result is identical to Eq. (21). Consequently, we have proven that, due to (infinitely fast) strong processes, one can ignore the subtleties related to different $\delta\mu$'s corresponding to subprocesses of $u + d \leftrightarrow u + s$. One rather may solely consider the rate Γ_d which is the sum of the rates of these subprocesses and a single $\delta\mu$ related to this rate. This is the method used in the main part of the paper.

APPENDIX C: DIRAC TRACES AND CONTRACTIONS

From the definitions (34) and (43) we find

$$\mathcal{T}^{00}(\hat{\mathbf{k}}, \hat{\mathbf{p}}) = 2(1 + \hat{\mathbf{k}} \cdot \hat{\mathbf{p}}), \quad (C1a)$$

$$\mathcal{T}^{0i}(\hat{\mathbf{k}}, \hat{\mathbf{p}}) = 2[\hat{k}^i + \hat{p}^i + i(\hat{\mathbf{k}} \times \hat{\mathbf{p}})^i], \quad (C1b)$$

$$\mathcal{T}^{i0}(\hat{\mathbf{k}}, \hat{\mathbf{p}}) = 2[\hat{k}^i + \hat{p}^i - i(\hat{\mathbf{k}} \times \hat{\mathbf{p}})^i], \quad (C1c)$$

$$\mathcal{T}^{ij}(\hat{\mathbf{k}}, \hat{\mathbf{p}}) = 2[\delta^{ij}(1 - \hat{\mathbf{k}} \cdot \hat{\mathbf{p}}) + \hat{k}^i \hat{p}^j + \hat{k}^j \hat{p}^i + i\epsilon^{ij\ell}(\hat{k}^\ell - \hat{p}^\ell)], \quad (C1d)$$

and

$$\mathcal{U}^{00}(\hat{\mathbf{k}}, \hat{\mathbf{p}}) = -2(1 + \hat{\mathbf{k}} \cdot \hat{\mathbf{p}}), \quad (C2a)$$

$$\mathcal{U}^{0i}(\hat{\mathbf{k}}, \hat{\mathbf{p}}) = 2[\hat{k}^i + \hat{p}^i + i(\hat{\mathbf{k}} \times \hat{\mathbf{p}})^i], \quad (C2b)$$

$$\mathcal{U}^{i0}(\hat{\mathbf{k}}, \hat{\mathbf{p}}) = -2[\hat{k}^i + \hat{p}^i - i(\hat{\mathbf{k}} \times \hat{\mathbf{p}})^i], \quad (C2c)$$

$$\mathcal{U}^{ij}(\hat{\mathbf{k}}, \hat{\mathbf{p}}) = 2[\delta^{ij}(1 - \hat{\mathbf{k}} \cdot \hat{\mathbf{p}}) + \hat{k}^i \hat{p}^j + \hat{k}^j \hat{p}^i + i\epsilon^{ij\ell}(\hat{k}^\ell - \hat{p}^\ell)]. \quad (C2d)$$

Consequently, we obtain the contractions

$$\mathcal{T}^{\mu\nu}(\hat{\mathbf{p}}_4, \hat{\mathbf{p}}_1)\mathcal{T}_{\mu\nu}(\hat{\mathbf{p}}_3, \hat{\mathbf{p}}_2) = 16(1 - \hat{\mathbf{p}}_4 \cdot \hat{\mathbf{p}}_3)(1 - \hat{\mathbf{p}}_1 \cdot \hat{\mathbf{p}}_2), \quad (C3a)$$

$$\begin{aligned} \mathcal{U}^{\nu\mu}(\hat{\mathbf{p}}_1, \hat{\mathbf{p}}_4)\mathcal{T}_{\mu\nu}(\hat{\mathbf{p}}_3, \hat{\mathbf{p}}_2) &= 8\{(1 - \hat{\mathbf{p}}_4 \cdot \hat{\mathbf{p}}_3)(1 - \hat{\mathbf{p}}_1 \cdot \hat{\mathbf{p}}_2) + (1 + \hat{\mathbf{p}}_1 \cdot \hat{\mathbf{p}}_3)(1 + \hat{\mathbf{p}}_4 \cdot \hat{\mathbf{p}}_2) - (1 + \hat{\mathbf{p}}_1 \cdot \hat{\mathbf{p}}_4)(1 + \hat{\mathbf{p}}_3 \cdot \hat{\mathbf{p}}_2) \\ &\quad - i[(\hat{\mathbf{p}}_3 + \hat{\mathbf{p}}_2) \cdot (\hat{\mathbf{p}}_1 \times \hat{\mathbf{p}}_4) + (\hat{\mathbf{p}}_1 + \hat{\mathbf{p}}_4) \cdot (\hat{\mathbf{p}}_2 \times \hat{\mathbf{p}}_3)]\}, \end{aligned} \quad (C3b)$$

$$\begin{aligned} \mathcal{U}^{\mu\nu}(\hat{\mathbf{p}}_4, \hat{\mathbf{p}}_1)\mathcal{T}_{\mu\nu}(\hat{\mathbf{p}}_3, \hat{\mathbf{p}}_2) &= 8\{(1 - \hat{\mathbf{p}}_4 \cdot \hat{\mathbf{p}}_3)(1 - \hat{\mathbf{p}}_1 \cdot \hat{\mathbf{p}}_2) + (1 + \hat{\mathbf{p}}_1 \cdot \hat{\mathbf{p}}_3)(1 + \hat{\mathbf{p}}_4 \cdot \hat{\mathbf{p}}_2) - (1 + \hat{\mathbf{p}}_1 \cdot \hat{\mathbf{p}}_4)(1 + \hat{\mathbf{p}}_3 \cdot \hat{\mathbf{p}}_2) \\ &\quad + i[(\hat{\mathbf{p}}_3 + \hat{\mathbf{p}}_2) \cdot (\hat{\mathbf{p}}_1 \times \hat{\mathbf{p}}_4) + (\hat{\mathbf{p}}_1 + \hat{\mathbf{p}}_4) \cdot (\hat{\mathbf{p}}_2 \times \hat{\mathbf{p}}_3)]\}. \end{aligned} \quad (C3c)$$

The imaginary terms in Eqs. (C3b) and (C3c) do not appear in the collision integral since they vanish after angular integration, see Appendix D 2.

APPENDIX D: ANGULAR INTEGRATION

In the first part of this appendix we compute the angular integrals in Eqs. (48) and (49). In the second part we show that the angular integral over the imaginary terms in Eqs. (C3b) and (C3c) vanishes.

1. Angular integration in Eqs. (48) and (49)

We have to compute

$$K \equiv \int d\Omega_1 \int d\Omega_2 \int d\Omega_3 \int d\Omega_4 (1 - \hat{\mathbf{p}}_1 \cdot \hat{\mathbf{p}}_2)(1 - \hat{\mathbf{p}}_3 \cdot \hat{\mathbf{p}}_4) \delta(\mathbf{p}_1 + \mathbf{p}_2 - \mathbf{p}_3 - \mathbf{p}_4). \quad (\text{D1})$$

One may start with the $d\Omega_2$ integral and rewrite the δ -function in terms of a modulus and an angular part

$$\delta[\mathbf{p}_2 - (\mathbf{p}_3 + \mathbf{p}_4 - \mathbf{p}_1)] = \frac{1}{p_2^2} \delta(p_2 - |\mathbf{p}_3 + \mathbf{p}_4 - \mathbf{p}_1|) \delta(\Omega_2 - \Omega), \quad (\text{D2})$$

where Ω stands for the angles of the vector $\mathbf{p}_3 + \mathbf{p}_4 - \mathbf{p}_1$. Thus, the effect of the angular δ -function is to replace the direction $\hat{\mathbf{p}}_2$ with $(\mathbf{p}_3 + \mathbf{p}_4 - \mathbf{p}_1)/|\mathbf{p}_3 + \mathbf{p}_4 - \mathbf{p}_1|$ (the numerator being actually p_2 because of the radial δ -function). Consequently, with $\mathbf{P} \equiv \mathbf{p}_3 + \mathbf{p}_4$ we obtain

$$K = \frac{1}{p_2^2} \int d\Omega_1 \int d\Omega_3 \int d\Omega_4 \left[1 - \frac{1}{p_2} (\hat{\mathbf{p}}_1 \cdot \mathbf{P} - p_1) \right] (1 - \hat{\mathbf{p}}_3 \cdot \hat{\mathbf{p}}_4) \delta(p_2 - |\mathbf{P} - \mathbf{p}_1|). \quad (\text{D3})$$

Next, we may straightforwardly perform the $d\Omega_1$ integration by choosing the z -axis to be parallel to \mathbf{P} . As in Ref. [39] we denote

$$p_{ij} \equiv |p_i - p_j|, \quad P_{ij} \equiv p_i + p_j. \quad (\text{D4})$$

Then,

$$\int d\Omega_1 \left[1 - \frac{1}{p_2} (\hat{\mathbf{p}}_1 \cdot \mathbf{P} - p_1) \right] \delta(p_2 - |\mathbf{P} - \mathbf{p}_1|) = \frac{\pi}{p_1^2} \frac{1}{P} \Theta(P - p_{12}) \Theta(P_{12} - P) (P_{12}^2 - P^2). \quad (\text{D5})$$

To obtain this result, note that $\Theta(a - |b|) = \Theta(a - b)\Theta(a + b)$. The remaining angular dependence is reduced to the angle between \mathbf{p}_3 and \mathbf{p}_4 , present in P . Hence, one integration, say $d\Omega_4$, is trivial while we are left with the azimuthal integral from $d\Omega_3$,

$$\begin{aligned} K &= \frac{8\pi^3}{p_1^2 p_2^2} \int_{-1}^1 dx \frac{1}{P} \Theta(P - p_{12}) \Theta(P_{12} - P) (P_{12}^2 - P^2) (1 - x) \\ &= \frac{4\pi^3}{p_1^2 p_2^2 p_3^2 p_4^2} \int_{p_{34}}^{P_{34}} dP \Theta(P - p_{12}) \Theta(P_{12} - P) (P_{12}^2 - P^2) (P_{34}^2 - P^2). \end{aligned} \quad (\text{D6})$$

Since $P_{ij} > p_{ij}$, there are four orders of $p_{12}, p_{34}, P_{12}, P_{34}$ that yield nonvanishing integrals,

$$p_{12} < p_{34} < P_{12} < P_{34}, \quad (\text{D7a})$$

$$p_{34} < p_{12} < P_{12} < P_{34}, \quad (\text{D7b})$$

$$p_{34} < p_{12} < P_{34} < P_{12}, \quad (\text{D7c})$$

$$p_{12} < p_{34} < P_{34} < P_{12}. \quad (\text{D7d})$$

The two other possibilities, $p_{12} < P_{12} < p_{34} < P_{34}$, and $p_{34} < P_{34} < p_{12} < P_{12}$ lead to vanishing integrals. Consequently,

$$K = \frac{4\pi^3}{p_1^2 p_2^2 p_3^2 p_4^2} L(p_{12}, P_{12}, p_{34}, P_{34}), \quad (\text{D8})$$

where we defined

$$\begin{aligned} L(a, b, c, d) &\equiv \Theta(c - a)\Theta(d - b)\Theta(b - c) J(c, b, b, d) + \Theta(a - c)\Theta(d - b) J(a, b, b, d) \\ &\quad + \Theta(a - c)\Theta(b - d)\Theta(d - a) J(a, d, b, d) + \Theta(c - a)\Theta(b - d) J(c, d, b, d), \end{aligned} \quad (\text{D9})$$

with

$$\begin{aligned} J(a, b, c, d) &\equiv \int_a^b dP (c^2 - P^2)(d^2 - P^2) \\ &= c^2 d^2 (b - a) - \frac{1}{3} (c^2 + d^2)(b^3 - a^3) + \frac{1}{5} (b^5 - a^5). \end{aligned} \quad (\text{D10})$$

With a simple relabeling of momenta we obtain the result for the other two terms in Eq. (49),

$$\int d\Omega_1 \int d\Omega_2 \int d\Omega_3 \int d\Omega_4 (1 + \hat{\mathbf{p}}_1 \cdot \hat{\mathbf{p}}_3)(1 + \hat{\mathbf{p}}_2 \cdot \hat{\mathbf{p}}_4) \delta(\mathbf{p}_1 + \mathbf{p}_2 - \mathbf{p}_3 - \mathbf{p}_4) = \frac{4\pi^3}{p_1^2 p_2^2 p_3^2 p_4^2} L(p_{24}, P_{24}, p_{13}, P_{13}), \quad (\text{D11})$$

and

$$\int d\Omega_1 \int d\Omega_2 \int d\Omega_3 \int d\Omega_4 (1 + \hat{\mathbf{p}}_1 \cdot \hat{\mathbf{p}}_4)(1 + \hat{\mathbf{p}}_2 \cdot \hat{\mathbf{p}}_3) \delta(\mathbf{p}_1 + \mathbf{p}_2 - \mathbf{p}_3 - \mathbf{p}_4) = \frac{4\pi^3}{p_1^2 p_2^2 p_3^2 p_4^2} L(p_{14}, P_{14}, p_{23}, P_{23}). \quad (\text{D12})$$

Consequently, with the definitions

$$I(p_1, p_2, p_3, p_4) \equiv L(p_{12}, P_{12}, p_{34}, P_{34}), \quad (\text{D13a})$$

$$\tilde{I}(p_1, p_2, p_3, p_4) \equiv L(p_{12}, P_{12}, p_{34}, P_{34}) + L(p_{24}, P_{24}, p_{13}, P_{13}) + L(p_{14}, P_{14}, p_{23}, P_{23}), \quad (\text{D13b})$$

we arrive at Eqs. (50) and (51).

2. Angular integration over imaginary terms in Eqs. (C3b) and (C3c)

Here, we show that the integral

$$I_0 \equiv \int d\Omega_1 \int d\Omega_2 \int d\Omega_3 \int d\Omega_4 [(\hat{\mathbf{p}}_2 + \hat{\mathbf{p}}_3) \cdot (\hat{\mathbf{p}}_1 \times \hat{\mathbf{p}}_4) + (\hat{\mathbf{p}}_1 + \hat{\mathbf{p}}_4) \cdot (\hat{\mathbf{p}}_2 \times \hat{\mathbf{p}}_3)] \delta(\mathbf{p}_1 + \mathbf{p}_2 - \mathbf{p}_3 - \mathbf{p}_4) \quad (\text{D14})$$

is zero. After integrating over one of the angles, say over Ω_2 , the scalar products containing a cross product can all be expressed in terms of one single scalar product,

$$I_0 = -\frac{1}{p_2^2} \left(1 + \frac{p_1 + p_3 + p_4}{p_2} \right) \int d\Omega_1 \int d\Omega_3 \int d\Omega_4 \hat{\mathbf{p}}_1 \cdot (\hat{\mathbf{p}}_3 \times \hat{\mathbf{p}}_4) \delta(p_2 - |\mathbf{p}_3 + \mathbf{p}_4 - \mathbf{p}_1|). \quad (\text{D15})$$

Let's consider the next integration, say over Ω_1 . The δ -function ensures that the distance of \mathbf{p}_1 to a fixed vector, namely $\mathbf{p}_3 + \mathbf{p}_4$, equals a fixed value, namely p_2 . So all allowed vectors \mathbf{p}_1 sit on a sphere around $\mathbf{p}_3 + \mathbf{p}_4$ with radius p_2 . The value of the integrand is given by the projection of \mathbf{p}_1 onto another fixed vector, namely $\hat{\mathbf{p}}_3 \times \hat{\mathbf{p}}_4$. Since this vector is orthogonal to $\mathbf{p}_3 + \mathbf{p}_4$, the integral over all these projections vanishes.

For the formal proof, one uses a frame with z -axis parallel to $\hat{\mathbf{p}}_3 \times \hat{\mathbf{p}}_4$ and an x -axis parallel to $\mathbf{p}_3 + \mathbf{p}_4$ (as above, $\mathbf{P} \equiv \mathbf{p}_3 + \mathbf{p}_4$),

$$\begin{aligned} \int d\Omega_1 \hat{\mathbf{p}}_1 \cdot (\hat{\mathbf{p}}_3 \times \hat{\mathbf{p}}_4) \delta(p_2 - |\mathbf{p}_3 + \mathbf{p}_4 - \mathbf{p}_1|) &= \int_0^\pi d\theta \sin \theta \cos \theta \int_0^{2\pi} d\varphi \delta(p_2 - \sqrt{P^2 + p_1^2 - 2Pp_1 \sin \theta \cos \varphi}) \\ &= \frac{2p_2}{Pp_1} \int_0^\pi d\theta \frac{\sin \theta}{|\sin \theta|} \cos \theta \left[1 - \left(\frac{p_2^2 + P^2 - p_1^2}{2Pp_1 \sin \theta} \right)^2 \right]^{-1/2} = 0, \end{aligned} \quad (\text{D16})$$

because the integrand is odd in θ over the integration range.

APPENDIX E: RATE FOR SMALL TEMPERATURES

In this appendix, we determine the leading contribution for the rates $\Gamma_d(0, \Delta, 0)$, $\Gamma_d(\Delta, 0, \Delta)$, $\Gamma_d(\Delta, \Delta, \Delta)$ at small temperatures. To this end, we analyse the following expression which originates from the Fermi distributions in the integrands of Eqs. (50) and (51) (prefactors are ignored since we only determine the leading contribution),

$$\begin{aligned} \Gamma_d(\Delta_1, \Delta_2, \Delta_4) &\sim \sum_{e_1 e_2 e_4} \left(e^{e_1 \sqrt{x_1^2 + \varphi_1^2}} + 1 \right)^{-1} \left(e^{e_2 \sqrt{x_2^2 + \varphi_2^2}} + 1 \right)^{-1} \\ &\quad \times \left(e^{-e_1 \sqrt{x_1^2 + \varphi_1^2} - e_2 \sqrt{x_2^2 + \varphi_2^2} + e_4 \sqrt{x_4^2 + \varphi_4^2} - y} + 1 \right)^{-1} \left(e^{-e_4 \sqrt{x_4^2 + \varphi_4^2}} + 1 \right)^{-1}, \end{aligned} \quad (\text{E1})$$

	$0 < \delta\mu < \Delta_0$	$\Delta_0 < \delta\mu < 2\Delta_0$	$2\Delta_0 < \delta\mu < 3\Delta_0$	$3\Delta_0 < \delta\mu$
$\Gamma_d(\Delta, \Delta, \Delta)$	$e^{-(2\Delta-\delta\mu)/T}$	$e^{-\Delta/T}$	$e^{-(3\Delta-\delta\mu)/T}$	1
$\Gamma_d(\Delta, 0, \Delta)$	$e^{-\Delta/T}$	$e^{-(2\Delta-\delta\mu)/T}$	1	1
$\Gamma_d(0, \Delta, 0)$	$e^{-(\Delta-\delta\mu)/T}$	1	1	1
$\Gamma_d(0, 0, 0)$	1	1	1	1

TABLE IV: Leading small temperature behavior of the rates with three, two, one, and zero gapped modes. A “1” indicates that the rate does not vanish at $T = 0$.

where $x_i \equiv (p_i - \mu_i)/T$, $\varphi_i \equiv \Delta(T)/T$, $y = \delta\mu/T$. This expression is integrated over x_1, x_2, x_4 , each ranging from $-\infty$ to ∞ (the lower boundary $-\infty$ actually being an approximation for $-\mu/T$). We perform the sum and, for small T (hence large φ_i), approximate

$$\begin{aligned} \Gamma_d(\Delta_1, \Delta_2, \Delta_4) \sim & \frac{1}{e^{\sqrt{x_4^2 + \varphi_4^2} - y} + e^{\sqrt{x_1^2 + \varphi_1^2} + \sqrt{x_2^2 + \varphi_2^2}}} + \frac{1}{e^{\sqrt{x_1^2 + \varphi_1^2} + \sqrt{x_4^2 + \varphi_4^2} - y} + e^{\sqrt{x_2^2 + \varphi_2^2}}} \\ & + \frac{1}{e^{\sqrt{x_2^2 + \varphi_2^2} + \sqrt{x_4^2 + \varphi_4^2} - y} + e^{\sqrt{x_1^2 + \varphi_1^2}}} + \frac{1}{e^{-y} + e^{\sqrt{x_1^2 + \varphi_1^2} + \sqrt{x_2^2 + \varphi_2^2} + \sqrt{x_4^2 + \varphi_4^2}}} \\ & + \frac{1}{e^{\sqrt{x_1^2 + \varphi_1^2} + \sqrt{x_2^2 + \varphi_2^2} + \sqrt{x_4^2 + \varphi_4^2} - y} + 1} + \frac{1}{e^{\sqrt{x_1^2 + \varphi_1^2} - y} + e^{\sqrt{x_2^2 + \varphi_2^2} + \sqrt{x_4^2 + \varphi_4^2}}} \\ & + \frac{1}{e^{\sqrt{x_2^2 + \varphi_2^2} - y} + e^{\sqrt{x_1^2 + \varphi_1^2} + \sqrt{x_4^2 + \varphi_4^2}}} + \frac{1}{e^{\sqrt{x_1^2 + \varphi_1^2} + \sqrt{x_2^2 + \varphi_2^2} - y} + e^{\sqrt{x_4^2 + \varphi_4^2}}}. \end{aligned} \quad (E2)$$

At this point, we distinguish between the different numbers of gapped modes. First, let us discuss the case $\varphi_1 = \varphi_2 = \varphi_3 \equiv \varphi$. We expand $\sqrt{x_i^2 + \varphi^2} \simeq \varphi + x_i^2/(2\varphi)$ and introduce the new (integration) variables $z_i = x_i/\sqrt{2\varphi}$,

$$\Gamma_d(\Delta, \Delta, \Delta) \sim \frac{1}{e^{\varphi-y} e^{z_1^2} + e^{2\varphi} e^{z_2^2+z_4^2}} + \frac{1}{e^{2\varphi-y} e^{z_1^2+z_2^2} + e^{\varphi} e^{z_4^2}} + \frac{1}{e^{-y} + e^{3\varphi} e^{z_1^2+z_2^2+z_4^2}} + \frac{1}{e^{3\varphi-y} e^{z_1^2+z_2^2+z_4^2} + 1}. \quad (E3)$$

Now note that for sufficiently small T , both φ and y have the same temperature dependence,

$$y = \frac{\delta\mu}{T}, \quad \varphi = \frac{\Delta(T)}{T} = \frac{\Delta_0}{T} \sqrt{1 - \left(\frac{T}{T_c}\right)^2} \rightarrow \frac{\Delta_0}{T}. \quad (E4)$$

Therefore, the limiting behavior of $\Gamma_d(\Delta, \Delta, \Delta)$ is different for the four cases $\delta\mu < \Delta_0$, $\Delta_0 < \delta\mu < 2\Delta_0$, $2\Delta_0 < \delta\mu < 3\Delta_0$, and $3\Delta_0 < \delta\mu$. In particular, the latter case leads to a nonzero value of Γ_d for $T \rightarrow 0$. This can be seen from Eq. (E3), where the 1 in the denominator of the fourth term on the right-hand side survives for $3\Delta_0 < \delta\mu$. We show the results for all four cases in the first row of Table IV.

Next, we consider the case $\varphi_1 = \varphi_4 \equiv \varphi$, $\varphi_2 = 0$. The analogue to Eq. (E3) is

$$\begin{aligned} \Gamma_d(\Delta, 0, \Delta) \sim & \frac{1}{e^{\varphi-y} e^{z_4^2} + e^{\varphi} e^{z_1^2+x_2}} + \frac{1}{e^{2\varphi-y} e^{z_1^2+z_4^2} + e^{x_2}} + \frac{1}{e^{\varphi-y} e^{x_2+z_4^2} + e^{\varphi} e^{z_1^2}} \\ & + \frac{1}{e^{-y} + e^{2\varphi} e^{z_1^2+x_2+z_4^2}} + \frac{1}{e^{2\varphi-y} e^{z_1^2+x_2+z_4^2} + 1} + \frac{1}{e^{-y} e^{x_2} + e^{2\varphi} e^{z_1^2+z_4^2}}. \end{aligned} \quad (E5)$$

Again, the results for different values of $\delta\mu$ are shown in Table IV.

Finally, for $\varphi_1 = \varphi_4 = 0$, $\varphi_2 \equiv \varphi$ we have

$$\begin{aligned} \Gamma_d(0, \Delta, 0) \sim & \frac{1}{e^{-y} e^{x_4} + e^{\varphi} e^{x_1+z_2^2}} + \frac{1}{e^{-y} e^{x_1+x_4} + e^{\varphi} e^{z_2^2}} + \frac{1}{e^{\varphi-y} e^{z_2^2+x_4} + e^{x_1}} \\ & + \frac{1}{e^{-y} + e^{\varphi} e^{x_1+z_2^2+x_4}} + \frac{1}{e^{\varphi-y} e^{x_1+z_2^2+x_4} + 1} + \frac{1}{e^{\varphi-y} e^{z_2^2} + e^{x_1+x_4}}. \end{aligned} \quad (E6)$$

Here, only for $\delta\mu < \Delta_0$, the rate goes to zero for $T \rightarrow 0$. The result is shown in the third row of Table IV. For completeness, we added the trivial result that for $\Gamma_d(0, 0, 0)$ the rate is nonzero at $T = 0$ for all $\delta\mu > 0$, see fourth row in Table IV.

- [2] D. Bailin and A. Love, Phys. Rept. **107**, 325 (1984).
- [3] J. Bardeen, L.N. Cooper, and J.R. Schrieffer, Phys. Rev. **108**, 1175 (1957).
- [4] For reviews, see K. Rajagopal and F. Wilczek, arXiv:hep-ph/0011333; M. G. Alford, Ann. Rev. Nucl. Part. Sci. **51**, 131 (2001) [arXiv:hep-ph/0102047]; G. Nardulli, Riv. Nuovo Cim. **25N3**, 1 (2002) [arXiv:hep-ph/0202037]; S. Reddy, Acta Phys. Polon. B **33**, 4101 (2002) [arXiv:nucl-th/0211045]; T. Schäfer, arXiv:hep-ph/0304281; D. H. Rischke, Prog. Part. Nucl. Phys. **52**, 197 (2004) [arXiv:nucl-th/0305030]; M. Alford, Prog. Theor. Phys. Suppl. **153**, 1 (2004) [arXiv:nucl-th/0312007]; M. Buballa, Phys. Rept. **407**, 205 (2005) [arXiv:hep-ph/0402234]; H. c. Ren, arXiv:hep-ph/0404074; M. Huang, Int. J. Mod. Phys. E **14**, 675 (2005) [arXiv:hep-ph/0409167]; I. A. Shovkovy, Found. Phys. **35**, 1309 (2005) [arXiv:nucl-th/0410091]. T. Schäfer, arXiv:hep-ph/0509068.
- [5] M. G. Alford, K. Rajagopal and F. Wilczek, Nucl. Phys. B **537**, 443 (1999) [arXiv:hep-ph/9804403].
- [6] K. Rajagopal and A. Schmitt, Phys. Rev. D **73**, 045003 (2006) [arXiv:hep-ph/0512043].
- [7] T. Schäfer, Phys. Rev. D **62**, 094007 (2000) [arXiv:hep-ph/0006034]; M. Buballa, J. Hosek and M. Oertel, Phys. Rev. Lett. **90**, 182002 (2003) [arXiv:hep-ph/0204275]; A. Schmitt, Q. Wang and D. H. Rischke, Phys. Rev. D **66**, 114010 (2002) [arXiv:nucl-th/0209050]; M. G. Alford, J. A. Bowers, J. M. Cheyne and G. A. Cowan, Phys. Rev. D **67**, 054018 (2003) [arXiv:hep-ph/0210106]; A. Schmitt, *Ph.D. dissertation*, arXiv:nucl-th/0405076; A. Schmitt, Phys. Rev. D **71**, 054016 (2005) [arXiv:nucl-th/0412033].
- [8] M. G. Alford, J. A. Bowers and K. Rajagopal, Phys. Rev. D **63**, 074016 (2001) [arXiv:hep-ph/0008208]; I. Giannakis and H. C. Ren, Phys. Lett. B **611**, 137 (2005) [arXiv:hep-ph/0412015]; R. Casalbuoni, R. Gatto, N. Ippolito, G. Nardulli and M. Ruggieri, Phys. Lett. B **627**, 89 (2005) [Erratum-ibid. B **634**, 565 (2006)] [arXiv:hep-ph/0507247]; M. Mannarelli, K. Rajagopal and R. Sharma, Phys. Rev. D **73**, 114012 (2006) [arXiv:hep-ph/0603076]; K. Rajagopal and R. Sharma, arXiv:hep-ph/0606066.
- [9] M. G. Alford, J. Berges and K. Rajagopal, Nucl. Phys. B **571**, 269 (2000) [arXiv:hep-ph/9910254]; A. Schmitt, Q. Wang and D. H. Rischke, Phys. Rev. Lett. **91**, 242301 (2003) [arXiv:nucl-th/0301090]; A. Schmitt, Q. Wang and D. H. Rischke, Phys. Rev. D **69**, 094017 (2004) [arXiv:nucl-th/0311006].
- [10] E. J. Ferrer, V. de la Incera and C. Manuel, Phys. Rev. Lett. **95**, 152002 (2005) [arXiv:hep-ph/0503162]; E. J. Ferrer, V. de la Incera and C. Manuel, Nucl. Phys. B **747**, 88 (2006) [arXiv:hep-ph/0603233].
- [11] I. A. Shovkovy and P. J. Ellis, Phys. Rev. C **66**, 015802 (2002) [arXiv:hep-ph/0204132].
- [12] G. W. Carter and S. Reddy, Phys. Rev. D **62**, 103002 (2000) [arXiv:hep-ph/0005228]; P. Jaikumar, M. Prakash and T. Schäfer, Phys. Rev. D **66**, 063003 (2002) [arXiv:astro-ph/0203088]; S. Reddy, M. Sadzikowski and M. Tachibana, Nucl. Phys. A **714**, 337 (2003) [arXiv:nucl-th/0203011]; J. Kundu and S. Reddy, Phys. Rev. C **70**, 055803 (2004) [arXiv:nucl-th/0405055]; R. Anglani, M. Mannarelli, G. Nardulli and M. Ruggieri, arXiv:hep-ph/0607341.
- [13] P. Jaikumar, C. D. Roberts and A. Sedrakian, Phys. Rev. C **73**, 042801 (2006) [arXiv:nucl-th/0509093].
- [14] A. Schmitt, I. A. Shovkovy and Q. Wang, Phys. Rev. D **73**, 034012 (2006) [arXiv:hep-ph/0510347].
- [15] Q. Wang, Z. g. Wang and J. Wu, arXiv:hep-ph/0605092.
- [16] B. A. Sa'd, I. A. Shovkovy and D. H. Rischke, arXiv:astro-ph/0607643.
- [17] A. Drago, A. Lavagno and G. Pagliara, Phys. Rev. D **71**, 103004 (2005) [arXiv:astro-ph/0312009].
- [18] M. Alford and K. Rajagopal, JHEP **0206**, 031 (2002) [arXiv:hep-ph/0204001].
- [19] A. W. Steiner, S. Reddy and M. Prakash, Phys. Rev. D **66**, 094007 (2002) [arXiv:hep-ph/0205201].
- [20] S. B. Rüster, V. Werth, M. Buballa, I. A. Shovkovy and D. H. Rischke, Phys. Rev. D **72**, 034004 (2005) [arXiv:hep-ph/0503184].
- [21] H. Abuki and T. Kunihiro, Nucl. Phys. A **768**, 118 (2006) [arXiv:hep-ph/0509172].
- [22] C. Manuel, A. Dobado and F. J. Llanes-Estrada, JHEP **0509**, 076 (2005) [arXiv:hep-ph/0406058].
- [23] K. D. Kokkotas and N. Andersson, arXiv:gr-qc/0109054.
- [24] N. Andersson, Astrophys. J. **502**, 708 (1998) [arXiv:gr-qc/9706075];
- [25] N. Andersson and G. L. Comer, Mon. Not. Roy. Astron. Soc. **328**, 1129 (2001) [arXiv:astro-ph/0101193].
- [26] For a lecture on r-mode instabilities see L. Lindblom, arXiv:astro-ph/0101136.
- [27] F. Weber, Prog. Part. Nucl. Phys. **54**, 193 (2005) [arXiv:astro-ph/0407155]; F. Weber, A. Torres i Cuadrat, A. Ho and P. Rosenfield, PoS **JHW2005**, 018 (2006) [arXiv:astro-ph/0602047].
- [28] C. Cutler and L. Lindblom, Astrophys. J. **314**, 234 (1987); R. F. Sawyer, Phys. Rev. D **39**, 3804 (1989).
- [29] Q. D. Wang and T. Lu, Phys. Lett. B **148**, 211 (1984).
- [30] P. Arnold, C. Dogan and G. D. Moore, arXiv:hep-ph/0608012.
- [31] P. Bhattacharyya, C.J. Pethick and H. Smith, Phys. Rev. B **15**, 3367 (1977); C.J. Pethick, P. Bhattacharyya and H. Smith, Phys. Rev. B **15**, 3384 (1977); D. Vollhardt and P. Wölfle, *The Superfluid Phases of Helium 3* (Taylor & Francis, London, 1990).
- [32] J. Madsen, Phys. Rev. D **46**, 3290 (1992).
- [33] J. D. Anand, N. Chandrika Devi, V. K. Gupta and S. Singh, Pramana **54**, 737 (2000).
- [34] P. Haensel, K. P. Levenfish and D. G. Yakovlev, Astron. Astrophys. **357**, 1157 (2000) [arXiv:astro-ph/0004183].
- [35] L. Lindblom and B. J. Owen, Phys. Rev. D **65**, 063006 (2002) [arXiv:astro-ph/0110558].
- [36] L. P. Kadanoff and G. Baym, *Quantum Statistical Mechanics* (Benjamin, New York, 1962).
- [37] M. Schönhofen, M. Cubero, B. L. Friman, W. Nörenberg and G. Wolf, Nucl. Phys. A **572**, 112 (1994).
- [38] A. Sedrakian and A. Dieperink, Phys. Lett. B **463**, 145 (1999) [arXiv:nucl-th/9905039].
- [39] A. Wadhwa, V.K. Gupta, S. Singh, and J.D. Anand, J. Phys. G **9**, 1137 (1995).
- [40] J. Madsen, Phys. Rev. D **47**, 325 (1993).
- [41] J. Madsen, Phys. Rev. Lett. **85**, 10 (2000) [arXiv:astro-ph/9912418].

- [42] S. B. Ruster, V. Werth, M. Buballa, I. A. Shovkovy and D. H. Rischke, Phys. Rev. D **73**, 034025 (2006) [arXiv:hep-ph/0509073].
- [43] L. Lindblom, J. E. Tohline and M. Vallisneri, Phys. Rev. Lett. **86**, 1152 (2001) [arXiv:astro-ph/0010653].
- [44] P. K. Sahu, G. F. Burgio and M. Baldo, Astrophys. J. **566**, L89 (2002) [arXiv:astro-ph/0111414]; P. Haensel, K. P. Levenfish and D. G. Yakovlev, Astron. Astrophys. **394**, 213 (2002) [arXiv:astro-ph/0208078]; M. E. Gusakov, D. G. Yakovlev and O. Y. Gnedin, Mon. Not. Roy. Astron. Soc. **361**, 1415 (2005) [arXiv:astro-ph/0502583].
- [45] M. Alford, M. Braby, S. Reddy, T. Schäfer, in preparation.